E-ISSN: 3023-784X

Advanced Radiology and Imaging

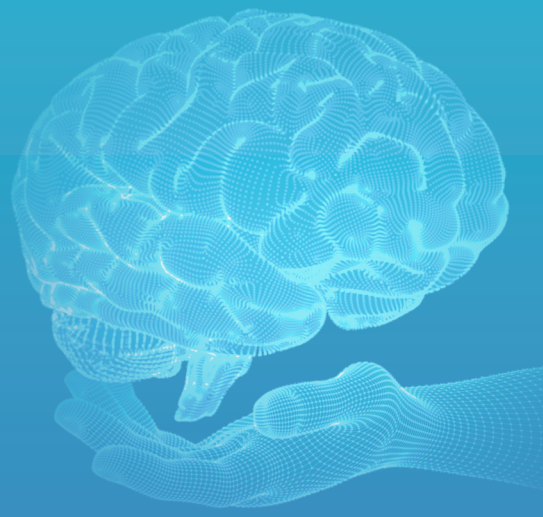

VOLUME 3 / ISSUE 2
AUGUST
2026

galenos Publishing House
ARI
advradiology.org

advradiology.org

Advanced Radiology and Imaging

VOLUME 3 / ISSUE 2
AUGUST 2026

EDITORIAL BOARD

VOLUME 3 / ISSUE 2
AUGUST
2026

Advanced Radiology and Imaging

advradiology.org

Please refer to the journal's webpage (**https://advradiology.org/**) for "**Journal Policy**" and "**Instructions to Authors**".

The editorial and publication process of the Advanced Radiology and Imaging are shaped in accordance with the guidelines of the **ICMJE, WAME, CSE, COPE, EASE,** and **NISO**. The journal is in conformity with the Principles of Transparency and Best Practice in Scholarly Publishing.

Advanced Radiology and Imaging is indexed in **Türkiye Citation Index, IdealOnline, Zenodo, Scilit, Index of Academic Documents, Gale, J-Gate, Türkmedline** and **Sudoc.**

The journal is published online.

Owner: Galenos Publishing House

Responsible Manager: Sonay Aydın

Publisher Contact
Address: Molla Gürani Mah. Kaçamak Sk. No: 21/1 34093 İstanbul, Türkiye
Phone: +90 (530) 177 30 97 / +90 (539) 307 32 03
E-mail: info@galenos.com.tr/yayin@galenos.com.tr
Web: www.galenos.com.tr
Publisher Certificate Number: 14521

Publication Date: August 2026
E-ISSN: 3023-784X
International scientific journal published quarterly.

advradiology.org

Advanced Radiology and Imaging

VOLUME 3 / ISSUE 2
AUGUST 2026

CONTENTS

Research Articles

RESEARCH ARTICLE

DOI: 10.4274/AdvRadiolImaging.galenos.2026.10820
Adv Radiol Imaging 2026;3(2):25-31

Ultrasonographic Markers of Perforated Appendicitis in Children: A Retrospective Diagnostic Accuracy Study

Ece Zengin[1], Elif Çiğdem Karataylı[2], Mehmet Emir Çevik[3], Hatice Kübra Özdemir[4], Tuğba Çaviş[5]

[1]*Tokat Gaziosmanpaşa University Faculty of Medicine, Department of Radiology, Tokat, Türkiye*
[2]*Kandıra Ecz. Kazım Dinç State Hospital, Clinic of Radiology, Kocaeli, Türkiye,*
[3]*Devrek State Hospital, Clinic of Radiology, Zonguldak, Türkiye*
[4]*University of Health Sciences Türkiye, Ankara Etlik City Hospital, Clinic of Radiology, Ankara, Türkiye*
[5]*University of Health Sciences Türkiye, Gülhane Training and Research Hospital, Radiology, Ankara, Türkiye*

Abstract

Objectives: Accurate preoperative differentiation between perforated and uncomplicated appendicitis in children remains challenging, but is essential for appropriate management. This study evaluated the diagnostic performance of predefined ultrasonographic signs and inflammatory markers at admission for differentiating perforated from uncomplicated appendicitis.

Methods: This retrospective diagnostic accuracy study included 174 pediatric patients who were evaluated with ultrasonography for suspected acute appendicitis. Final reference diagnoses were: no appendicitis (normal appendix) (n=55), simple appendicitis (n=82), and perforated appendicitis (n=37). The sonographic variables included loculated periappendiceal fluid, appendicolith, complex free fluid, periappendiceal fat echogenicity, distribution of free fluid in five abdominal regions, and periportal echogenicity. Leukocyte count, erythrocyte sedimentation rate (ESR), and C-reactive protein (CRP) were recorded at admission. Diagnostic performance was calculated for perforated versus simple appendicitis.

Results: Children with perforated appendicitis were younger than those with simple appendicitis or no appendicitis/normal appendix. ESR and CRP levels were highest in the perforated group ($p<0.001$). Loculated periappendiceal fluid was observed in 18 of 37 perforated cases and 7 of 82 simple cases, yielding 48.6% sensitivity and 91.5% specificity ($p<0.001$). Complex free fluid had a sensitivity of 51.4% and a specificity of 87.8% ($p<0.001$). Echogenic periappendiceal fat occurred frequently in both appendicitis groups and was not specific to perforation.

Conclusion: Loculated periappendiceal fluid and complex free fluid are specific but incompletely sensitive sonographic signs of perforated appendicitis in children. CRP and ESR reflect the severity of inflammation and should be interpreted together with ultrasound findings, rather than as isolated diagnostic tests.

Keywords: Appendicitis, child, ultrasonography, C-reactive protein, perforation, erythrocyte sedimentation rate

Introduction

Acute appendicitis is a common reason for emergency abdominal surgery in children. Diagnosis is less straightforward in younger patients because abdominal pain may be poorly localized and overlap with gastroenteritis, mesenteric lymphadenitis, urinary tract infection, or gynecologic disease.[1,2] Detecting perforation at initial assessment is important because perforated appendicitis is associated with abscess formation, peritonitis, prolonged hospitalization, broader antibiotic use, and increased resource utilization.[3,4]

Ultrasonography is commonly used initially in children with suspected appendicitis because it avoids ionizing radiation and can be repeated at the bedside or in the radiology suite.[2,5-9] In uncomplicated appendicitis, the expected finding is a blind-ending, non-compressible, enlarged tubular appendix arising from the cecum, often accompanied by adjacent inflammatory change.[5,9]

Perforation changes this appearance. The appendix may decompress, collapse, or become indistinct within phlegmon, bowel gas, inflamed fat, or fluid. In that setting, failure to show a clearly enlarged appendix is not reassuring when secondary inflammatory signs are present.[10-16]

Secondary signs associated with perforated or complicated appendicitis include loculated periappendiceal fluid or abscess, complex free fluid, appendicolith, free fluid beyond the right lower quadrant, bowel dilatation, mural disruption or loss of stratification, and marked periappendiceal fat echogenicity.[10-16] Prior pediatric studies show a

Cite this article as: Zengin E, Karataylı EÇ, Çevik ME, Özdemir HK, Çaviş T. Ultrasonographic markers of perforated appendicitis in children: a retrospective diagnostic accuracy study. Adv Radiol Imaging. 2026;3(2):25-31

Address for Correspondence: Ece Zengin MD, Tokat Gaziosmanpaşa University, Department of Radiology, Tokat, Türkiye
E-mail: drecezengin@hotmail.com ORCID ID: orcid.org/0009-0005-1488-6820
Received: 08.07.2026 Accepted: 30.07.2026 Published: 31.08.2026

consistent pattern: these signs tend to be specific but not sufficiently sensitive; their absence does not exclude perforation.[11-16] The presence of an appendicolith is associated with prolonged symptoms and a higher risk of perforation, although its value as a single diagnostic sign varies across cohorts.[17]

Inflammatory markers such as C-reactive protein (CRP), erythrocyte sedimentation rate (ESR), and leukocyte count may help grade disease severity, but individual blood tests do not reliably separate complicated from uncomplicated appendicitis.[18-20] Recent work supports a combined interpretation of clinical, laboratory, and imaging findings rather than reliance on a single variable.[21-23] This study assessed selected ultrasound findings and admission inflammatory markers to differentiate perforated appendicitis, simple appendicitis, and no appendicitis in children.

Methods

Study Design and Patients

This retrospective, observational diagnostic accuracy study was prepared in accordance with STARD 2015 and STROBE reporting guidelines, where applicable.[24,25] Ethical approval for the retrospective review was obtained from Erzincan Binali Yıldırım University Institutional Ethics Committee (approval number: E-16377862.09.AK-16, date: 25.06.2026). The requirement for written informed consent was waived because of the retrospective design.

Medical records, laboratory data, ultrasonography reports, archived sonographic images, when available, operative notes, histopathology reports, and final clinical outcomes were reviewed for pediatric patients who were evaluated for suspected acute appendicitis.

A total of 244 pediatric patients were screened. Patients were eligible if abdominal ultrasonography had been performed during the initial diagnostic work-up and a final pathological or clinical outcome was available. Seventy patients were excluded for the following reasons: preoperative ultrasonography was unavailable; the ultrasonography report lacked sufficient information on predefined sonographic findings; relevant laboratory, operative, or histopathological data were missing; the final diagnosis could not be verified; or an appropriate reference standard could not be established. The remaining 174 patients were included in the final analysis and classified into three reference groups: no appendicitis (normal appendix), simple appendicitis, and perforated appendicitis (Figure 1).

Laboratory Parameters

Admission leukocyte count (age-dependent reference range for children aged 2-15 years: 4.5-17.0×10^9/L), CRP (reference range: 0-5 mg/L), and ESR (reference range: 0-20 mm/h) were obtained from the hospital database. These variables were compared across the three final diagnostic groups.

Ultrasonographic Evaluation

All ultrasonographic examinations during routine clinical care of children referred for suspected appendicitis were performed using a GE LOGIQ E9 ultrasound system (GE Healthcare, USA). A 5-8 MHz convex transducer was used for the initial abdominal survey; a 5-12 MHz linear transducer was then used for graded-compression evaluation of the appendix. Examinations were performed by one of two radiologists with 10 and 5 years' experience in pediatric ultrasonography.

The predefined sonographic variables included loculated periappendiceal fluid collection, appendicolith, complex free fluid, increased periappendiceal fat echogenicity, free-fluid distribution in the abdominal recesses, and increased periportal echogenicity. Complex free fluid was defined as intraperitoneal fluid containing internal echoes, debris, or heterogeneous echogenic material. Loculated periappendiceal fluid was defined as a localized fluid collection adjacent to the appendix or the expected appendiceal region, and increased periappendiceal fat echogenicity was defined as a focal hyperechoic inflammatory change surrounding the appendix or within the right lower quadrant. For free-fluid distribution, the abdomen was divided into the right upper, left upper, right lower, and left lower quadrants and the pelvis; involvement was categorized as 1-2, 3-4, or all 5 regions.

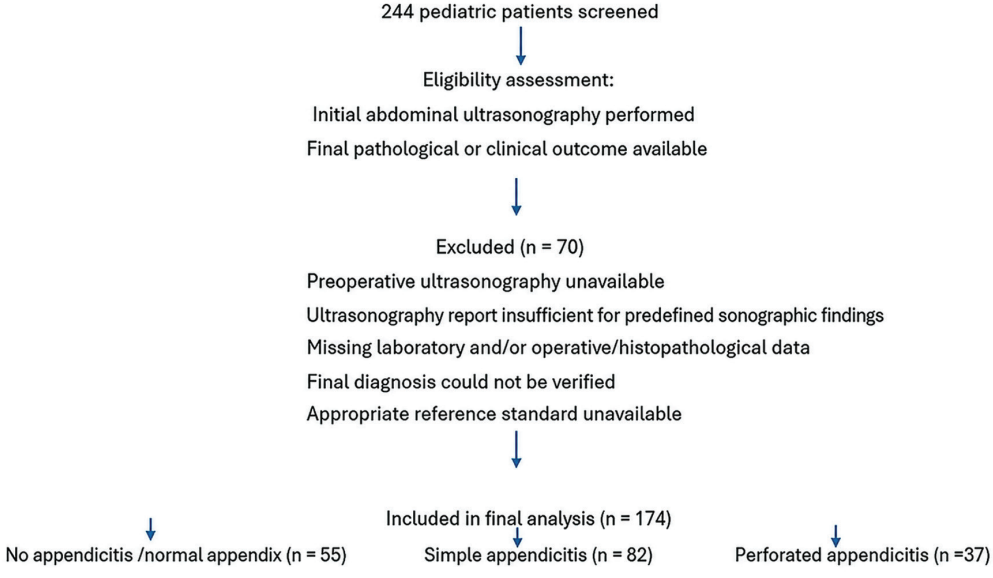

Figure 1. Workflow for the study

Study variables were extracted from the original radiology reports and, when available, archived ultrasonographic images. Archived images were reviewed jointly by the same two radiologists, who were blinded to the operative and histopathological findings. Final image interpretation was reached by consensus; therefore, interobserver agreement was not assessed.

Reference Standard

The final diagnosis was established by histopathological examination for patients who underwent appendectomy, and by final clinical diagnosis for patients managed nonoperatively. Simple appendicitis was defined as appendiceal inflammation without perforation, periappendiceal abscess, phlegmon, or transmural defect. Perforated appendicitis was defined as pathological confirmation of perforation or operative evidence of perforation, periappendiceal abscess, or phlegmon. Patients without appendicitis were assigned to the no-appendicitis/normal-appendix group based on histopathological findings or the final clinical diagnosis.

Statistical Analysis

Continuous variables are presented as mean ± standard deviation, and categorical variables as counts and percentages. Normality was assessed using the Shapiro-Wilk test. Comparisons among the three diagnostic groups were performed using ANOVA for normally distributed variables or the Kruskal-Wallis test for non-normally distributed variables. When overall group differences were significant, post-hoc pairwise comparisons were performed using the Bonferroni correction. Categorical variables were compared using the chi-square test or Fisher's exact test.

Receiver operating characteristic (ROC) curve analysis was performed to evaluate the diagnostic performance of CRP, ESR, and leukocyte count for identifying perforated appendicitis. The area under the ROC curve (AUC), optimal cut-off values, sensitivity, specificity, positive predictive value (PPV), negative predictive value (NPV), and 95% confidence intervals (CIs) were calculated.

The diagnostic performance of predefined sonographic findings for differentiating perforated from simple appendicitis was assessed by calculating sensitivity, specificity, PPV, NPV, and 95% CIs. Cis for sensitivity and specificity were estimated using the Wilson score method. P values for sonographic findings were calculated using two-sided Fisher exact tests. A two-sided p value <0.05 was considered statistically significant. Statistical analyses were performed using IBM SPSS Statistics (version 30; IBM Corp., Armonk, NY, USA).

Results

Patient Characteristics

Between January 2024 and March 2026, a total of 174 pediatric patients aged 2-15 years who were evaluated for suspected acute appendicitis were included in the study. The final reference diagnoses were: no appendicitis (normal appendix) in 55 patients, simple appendicitis in 82 patients, and perforated appendicitis in 37 patients (Table 1).

The cohort comprised 108 boys (62.1%) and 66 girls (37.9%), with a mean age of 7.3±2.7 years. Patients with perforated appendicitis were significantly younger than those with simple appendicitis or a normal appendix (no appendicitis). Mean age was 8.3±2.9 years in the no appendicitis/normal appendix group, 7.2±2.5 years in the simple appendicitis group, and 6.0±2.7 years in the perforated appendicitis group (p=0.018).Sex distribution did not differ significantly among the three groups (p=0.214).

Laboratory Findings

Mean leukocyte count was $10.7\pm2.7\times10^3/\mu L$ in the no appendicitis/normal appendix group, $13.0 \pm 3.2 \times10^3/\mu L$ in the simple appendicitis group, and $14.1\pm2.8\times10^3/\mu L$ in the perforated appendicitis group. Mean ESR values were 6.5±2.2 mm/h, 18.4±3.8 mm/h, and 25.8±5.0 mm/h, respectively. Mean CRP levels were 2.8±1.2 mg/L, 31.1±5.9 mg/L, and 134.5±10.8 mg/L, respectively (Table 2).

Comparisons among the three diagnostic groups revealed significant differences in age, CRP, and ESR (all p<0.05). Post-hoc pairwise comparisons with Bonferroni correction showed that CRP and ESR levels were significantly higher in the perforated appendicitis group than in both the simple appendicitis group and the no appendicitis/normal appendix group (both p<0.001). In contrast, the leukocyte count was higher in both appendicitis groups than in the no appendicitis/normal appendix group, but it did not differ significantly between simple and perforated appendicitis after Bonferroni correction.

ROC curve analysis demonstrated that CRP had the highest diagnostic performance for discriminating perforated appendicitis, followed by ESR, while leukocyte count had limited discriminatory ability. The AUCs, 95% CIs, optimal cut-off values, sensitivities, and specificities are summarized in Table 3.

Ultrasonographic Findings

The distribution of sonographic findings is summarized in Table 4. A normal appendix was directly visualized in 41 of the 55 patients (74.5%) in the no appendicitis/normal appendix group. Among the remaining patients, no secondary signs of appendicitis, such as increased mesenteric echogenicity or free fluid, were identified, and appendicitis was excluded based on symptom resolution and an uneventful clinical follow-up lasting at least 30 days.

An appendicolith was identified in 15 patients with perforated appendicitis and in 22 patients with simple appendicitis, and was not significantly associated with perforation (p=0.142).

Increased periappendiceal fat echogenicity was observed in 34 patients with perforated appendicitis and in 73 patients with simple appendicitis (p=0.752).

Loculated periappendiceal fluid was detected in 18 of 37 patients with perforated appendicitis, compared with 7 of 82 patients with simple appendicitis (p<0.001) and was not observed in the no-appendicitis/normal-appendix group (Figure 2).

Fluid involving one or two abdominal regions occurred with similar frequency in the simple appendicitis and perforated appendicitis groups (p=0.843). Fluid involving all five abdominal regions was observed in 7 patients with perforated appendicitis, 7 with simple appendicitis, and 1 patient in the no-appendicitis/normal-appendix group (p=0.128).

Complex free fluid was present in 19 patients with perforated appendicitis, 10 with simple appendicitis (p<0.001), and 5 with no appendicitis/normal appendix (Figure 3).

Periportal echogenicity was recorded in 8 patients with no appendicitis/normal appendix, 46 with simple appendicitis, and 11 with perforated appendicitis (Figure 4).

To differentiate perforated from simple appendicitis, loculated periappendiceal fluid and complex free fluid were the most specific sonographic findings. Loculated periappendiceal fluid had a sensitivity of 48.6% and specificity of 91.5%, whereas complex free fluid had a sensitivity of 51.4% and specificity of 87.8%.

Fluid involving all five abdominal regions also demonstrated high specificity (91.5%) but low sensitivity (18.9%). In contrast, increased periappendiceal fat echogenicity demonstrated high sensitivity (91.9%) but poor specificity (11.0%) for differentiating perforated from simple appendicitis. Periportal echogenicity was significantly more frequent in simple appendicitis than in perforated appendicitis (p=0.010) and showed limited discriminatory performance when considered as an isolated finding (Table 5).

Discussion

In this pediatric cohort, loculated periappendiceal fluid and complex free fluid were the strongest ultrasound indicators of perforated appendicitis. Both signs were specific, but only moderately sensitive. This pattern is clinically useful: when present, these findings should raise suspicion of perforation; when absent, perforation cannot be excluded.

Table 1. Distribution of patients according to final diagnosis

	No appendicitis/normal appendix (n=55)	Simple appendicitis (n=82)	Perforated appendicitis (n=37)	p value
Number of patients	55	82	37	-
Age, years, mean ± SD	8.3±2.9	7.2±2.5	6.0±2.7	0.018
Sex, n (%)				0.214
Male	39 (70.9)	49 (59.8)	20 (54.1)	
Female	16 (29.1)	33 (40.2)	17 (45.9)	

Data are presented as mean ± SD or number of patients (%). P values were calculated using ANOVA for age and the chi-square test for sex distribution
SD: Standard deviation

Table 2. Laboratory findings and diagnostic performance of inflammatory markers

Parameter	No appendicitis/normal appendix (n=55)	Simple appendicitis (n=82)	Perforated appendicitis (n=37)	Overall p value
Leukocyte count (×10³/μL)	10.7±2.7	13.0±3.2	14.1±2.8	NS†
ESR (mm/h)	6.5±2.2	18.4±3.8	25.8±5.0	<0.001*
CRP (mg/L)	2.8±1.2	31.1±5.9	134.5±10.8	<0.001*

Data are presented as mean ± standard deviation. *: Overall comparison among the three groups.
†: Leukocyte count differed between the appendicitis and no appendicitis groups but not between simple and perforated appendicitis on Bonferroni post-hoc analysis
CRP: C-reactive protein, ESR: Erythrocyte sedimentation rate

Table 3. Laboratory findings and diagnostic performance of inflammatory markers

Variable	AUC (95% CI)	Cut-off	Sensitivity
CRP	0.88 (0.82-0.94)	52 mg/L	86.5%
ESR	0.79 (0.71-0.87)	21 mm/h	74.3%
Leukocyte count	0.67 (0.58-0.76)	13.8 ×10³/μL	65.2%

Cut-off values were determined from ROC curve analysis
AUC: Area under the curve, CI: Confidence interval, CRP: C-reactive protein, ESR: Erythrocyte sedimentation rate, ROC: Receiver operating characteristic

Table 4. Distribution of ultrasonographic findings according to final diagnosis

US finding	No appendicitis/normal appendix (n=55)	Simple appendicitis (n=82)	Perforated appendicitis (n=37)
Loculated periappendiceal fluid	0 (0.0%)	7 (8.5%)	18 (48.6%)
Appendicolith	0 (0.0%)	22 (26.8%)	15 (40.5%)
Complex free fluid	5 (9.1%)	10 (12.2%)	19 (51.4%)
Echogenic periappendiceal fat	6 (10.9%)	73 (89.0%)	34 (91.9%)
Fluid involving 1-2 abdominal regions	29 (52.7%)	43 (52.4%)	18 (48.6%)
Fluid involving 3-4 abdominal regions	5 (9.1%)	22 (26.8%)	12 (32.4%)
Fluid involving all 5 abdominal regions	1 (1.8%)	7 (8.5%)	7 (18.9%)
Periportal echogenicity	8 (14.5%)	46 (56.1%)	11 (29.7%)

Data are presented as n and percentage (%)
US: Ultrasonography

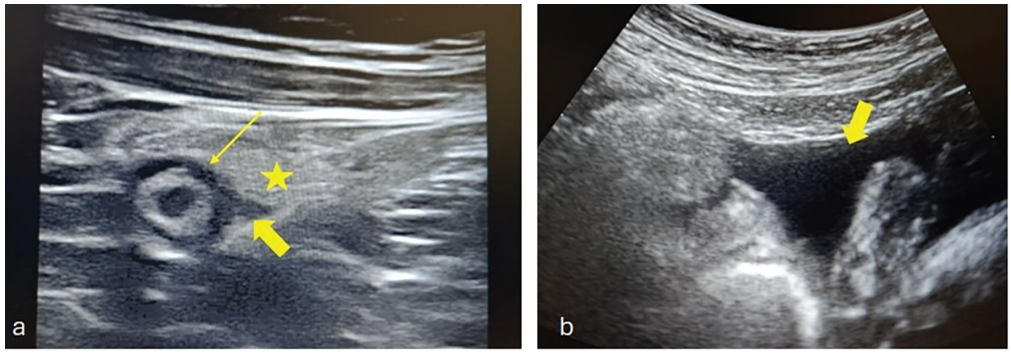

Figure 2. **a)** Linear transducer (5-12 MHz). Dilated inflamed appendix (thin arrow), small loculated periappendiceal fluid (thick arrow), and increased echogenicity of the adjacent mesenteric fat (asterisk) in a patient with simple appendicitis. **b)** Curvilinear transducer (5-8 MHz). Free pelvic fluid (thick arrow) in another patient with simple appendicitis; the appendix was not visualized

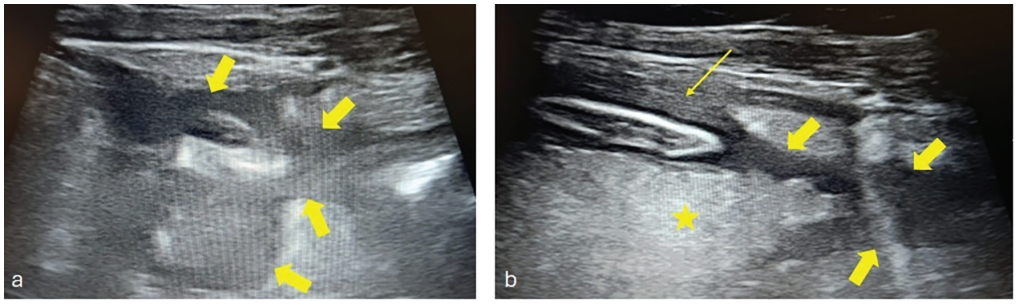

Figure 3. **a)** Linear transducer with wide view (5-12 MHz). Complex free fluid in the right lower quadrant (thick arrows). **b)** Same patient. Dilated inflamed appendix (thin arrow), adjacent hyperechoic mesenteric fat (asterisk), and complex free fluid (thick arrows). The patient had perforated appendicitis with purulent intra-abdominal fluid at surgery

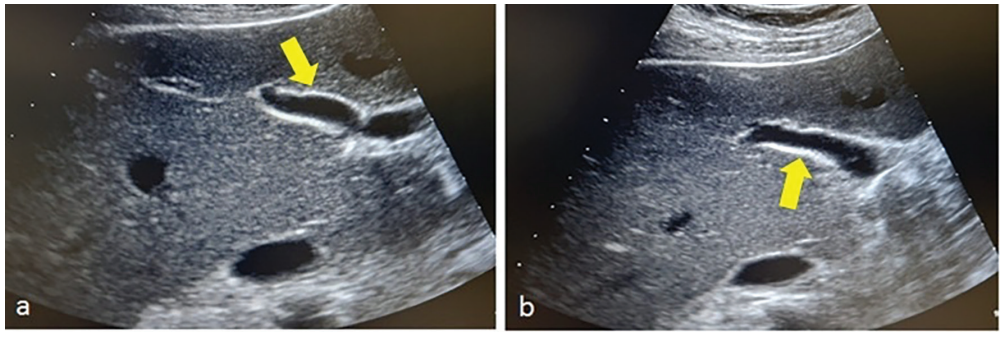

Figure 4. **a** and **b)** Curvilinear transducer (5-8 MHz). Images from the same patient demonstrate increased periportal echogenicity

Table 5. Diagnostic performance of ultrasonographic findings for differentiating perforated from simple appendicitis

Ultrasonographic finding	Sensitivity (%)	Specificity (%)	PPV (%)	NPV (%)	p value
Appendicolith	40.5	73.2	40.5	73.2	0.142
Echogenic periappendiceal fat	91.9	11.0	31.8	75.0	0.752
Loculated periappendiceal fluid	48.6	91.5	72.0	79.8	<0.001
Fluid involving 1-2 abdominal regions	48.6	47.6	29.5	67.2	0.843
Fluid involving 3-4 abdominal regions	32.4	73.2	35.3	70.6	0.661
Fluid involving all 5 abdominal regions	18.9	91.5	50.0	71.4	0.128
Complex free fluid	51.4	87.8	65.5	80.0	<0.001
Periportal echogenicity	29.7	43.9	19.3	58.1	0.010

P values were calculated using two-sided Fisher exact tests for perforated versus simple appendicitis
PPV: Positive predictive value, NPV: Negative predictive value

The results agree with previous pediatric imaging studies showing that ultrasound has limited sensitivity but good specificity for complicated or perforated appendicitis.[10-16,21,22] Once perforation occurs, the appendix may decompress or become obscured by inflammatory change; the diagnosis then depends on secondary signs rather than direct visualization of a wall defect. Previous studies have also found that combinations of secondary signs improve specificity and that complex periappendiceal fluid is an important sign.[11,12]

Periappendiceal fat echogenicity was frequent in both simple and perforated appendicitis. It is a useful sign of local inflammation, but in this dataset, it did not classify disease severity. This distinction matters because echogenic fat is often conspicuous on ultrasound and can be overinterpreted if evaluated without consideration of fluid characteristics, abscess, appendicolith, and clinical context.

An appendicolith was more frequent in perforated appendicitis, but its diagnostic performance in isolation was modest. The finding remains clinically relevant because appendicoliths have been associated with prolonged symptoms and a higher risk of perforation, but it should not be treated as a standalone marker of perforation.[17]

CRP and ESR were higher in perforated appendicitis, whereas leukocyte count did not clearly differentiate simple from perforated appendicitis. Individual blood biomarkers alone are not sufficiently accurate to diagnose complicated appendicitis.[18-20] Interpretation should therefore combine ultrasound findings, clinical assessment, and inflammatory markers.[21-23]

In the report, loculated periappendiceal fluid or complex free fluid should be explicitly communicated as findings that increase concern for perforation. These findings may affect the urgency of surgical consultation, antibiotic planning, and the search for an abscess or diffuse peritoneal fluid. In contrast, echogenic periappendiceal fat alone should be reported as inflammatory change, but not as proof of perforation.

Study Limitations

This study has several limitations. Its retrospective single-center design may limit the generalizability of the findings and introduce selection bias. In addition, ultrasonography is inherently operator-dependent, and image acquisition may have varied despite examinations being performed by experienced pediatric radiologists. Furthermore, archived ultrasound images were not available for all patients, and image interpretation was therefore based on the stored images and reports. The relatively small number of patients with perforated appendicitis may also have limited the statistical power for evaluating some secondary sonographic findings. Although several secondary sonographic findings, particularly loculated periappendiceal fluid and fluid involving all five abdominal regions, demonstrated high specificity for perforation, their sensitivities were relatively low. Therefore, the absence of these findings should not be considered sufficient to exclude perforation. Rather, secondary sonographic findings should be interpreted collectively and in conjunction with primary ultrasonographic findings, laboratory markers, and the overall clinical presentation. Prospective multicenter studies with larger patient cohorts are warranted to validate these findings.

Conclusion

Loculated periappendiceal fluid and complex free fluid are specific sonographic signs of perforated appendicitis in children; however, their sensitivity is limited. Periappendiceal fat echogenicity supports the presence of appendiceal inflammation, but does not reliably distinguish perforated from simple appendicitis. CRP and ESR provide information on disease severity when interpreted alongside ultrasound findings. A combined clinical, laboratory, and imaging assessment remains necessary for the preoperative evaluation of suspected appendiceal perforation in pediatric patients.

Ethics

Ethics Committee Approval: Ethical approval for the retrospective review was obtained from Erzincan Binali Yıldırım University Institutional Ethics Committee (approval number: E-16377862.09.AK-16, date: 25.06.2026).

Informed Consent: Since the study was a retrospective study, informed consent was not required by the ethics committee.

Footnotes

Authorship Contributions

Surgical and Medical Practices: E.Z., E.Ç.K., Concept: E.Z., M.E.Ç., Design: E.Z., E.Ç.K., Data Collection or Processing: E.Z., E.Ç.K., M.E.Ç., Analysis or Interpretation: E.Z., M.E.Ç., Literature Search: E.Z., M.E.Ç., H.K.Ö., T.Ç., Writing: E.Z., E.Ç.K., H.K.Ö., T.Ç.

Conflict of Interest: No conflict of interest was declared by the authors.

Financial Disclosure: The authors declared that this study received no financial support.

References

1. Shogilev DJ, Duus N, Odom SR, Shapiro NI. Diagnosing appendicitis: evidence-based review of the diagnostic approach in 2014. West J Emerg Med. 2014;15:859-71.
2. Di Saverio S, Podda M, De Simone B, et al. Diagnosis and treatment of acute appendicitis: 2020 update of the WSES Jerusalem guidelines. World J Emerg Surg. 2020;15:27.
3. Narsule CK, Kahle EJ, Kim DS, Anderson AC, Luks FI. Effect of delay in presentation on rate of perforation in children with appendicitis. Am J Emerg Med. 2011;29:890-3.
4. Yousef Y, Youssef F, Dinh T, et al. Risk stratification in pediatric perforated appendicitis: Prospective correlation with outcomes and resource utilization. J Pediatr Surg. 2018;53:250-5.
5. Puylaert JB. Acute appendicitis: US evaluation using graded compression. Radiology. 1986;158:355-60.
6. Doria AS, Moineddin R, Kellenberger CJ, et al. US or CT for diagnosis of appendicitis in children and adults? A meta-analysis. Radiology. 2006;241:83-94.
7. Strouse PJ. Pediatric appendicitis: an argument for US. Radiology. 2010;255:8-13.
8. Expert Panel on Pediatric Imaging:; Koberlein GC, Trout AT, Rigsby CK, et al. ACR Appropriateness Criteria® Suspected Appendicitis-Child. J Am Coll Radiol. 2019;16:S252-63.
9. Sivit CJ, Siegel MJ, Applegate KE, Newman KD. When appendicitis is suspected in children. Radiographics. 2001;21:247-62; questionnaire 288-94.
10. Quigley AJ, Stafrace S. Ultrasound assessment of acute appendicitis in paediatric patients: methodology and pictorial overview of findings seen. Insights Imaging. 2013;4:741-51.
11. Tulin-Silver S, Babb J, Pinkney L, et al. The challenging ultrasound diagnosis of perforated appendicitis in children: constellations of sonographic findings improve specificity. Pediatr Radiol. 2015;45:820-30.

12. Carpenter JL, Orth RC, Zhang W, Lopez ME, Mangona KL, Guillerman RP. Diagnostic performance of US for differentiating perforated from nonperforated pediatric appendicitis: a prospective cohort study. Radiology. 2017;282:835-41.
13. Gonzalez DO, Lawrence AE, Cooper JN, et al. Can ultrasound reliably identify complicated appendicitis in children? J Surg Res. 2018;229:76-81.
14. Rawolle T, Reismann M, Minderjahn MI, et al. Sonographic differentiation of complicated from uncomplicated appendicitis. Br J Radiol. 2019;92:20190102.
15. Tong L, Nataraja RM, VanHaltren K, Sulaksana TH, Vinycomb TI, Pacilli M. The utility of sonographic signs to diagnose simple and complicated appendicitis in children. Pediatr Surg Int. 2023;39:114.
16. Badlis M, Amari K, Alkheshi M, Alolaby K, Alsaid B. Ultrasound and computed tomography in differentiating between simple and complicated appendicitis in pediatric patients. Pediatr Surg Int. 2024;40:299.
17. Yoon HM, Kim JH, Lee JS, Ryu JM, Kim DY, Lee JY. Pediatric appendicitis with appendicolith often presents with prolonged abdominal pain and a high risk of perforation. World J Pediatr. 2018;14:184-90.
18. Bröker ME, van Lieshout EM, van der Elst M, Stassen LP, Schepers T. Discriminating between simple and perforated appendicitis. J Surg Res. 2012;176:79-83.
19. Sikander B, Rosenberg J, Fonnes S. Individual biomarkers in the blood are not yet applicable in diagnosing complicated appendicitis: a scoping review. Am J Emerg Med. 2023;67:100-7.
20. Ha SC, Tsai YH, Koh CC, Hong SG, Chen Y, Yao CL. Blood biomarkers to distinguish complicated and uncomplicated appendicitis in pediatric patients. J Formos Med Assoc. 2024;123:1093-8.
21. Nijssen DJ, van Amstel P, van Schuppen J, Eeftinck Schattenkerk LD, Gorter RR, Bakx R. Accuracy of ultrasonography for differentiating between simple and complex appendicitis in children. Pediatr Surg Int. 2021;37:843-9.
22. Bolmers MDM, Bom WJ, Scheijmans JCG, et al. Accuracy of imaging in discriminating complicated from uncomplicated appendicitis in daily clinical practice. Int J Colorectal Dis. 2022;37:1385-91.
23. Banerjee A, Ratan SK, Neogi S, Goswami B, Dixit R, Panda SS. Role of ultrasonography and inflammatory markers in predicting complicated appendicitis. J Indian Assoc Pediatr Surg. 2022;27:448-54.
24. Bossuyt PM, Reitsma JB, Bruns DE, et al. STARD 2015: an updated list of essential items for reporting diagnostic accuracy studies. BMJ. 2015;351:h5527.
25. von Elm E, Altman DG, Egger M, et al. The Strengthening the Reporting of Observational Studies in Epidemiology (STROBE) statement: guidelines for reporting observational studies. J Clin Epidemiol. 2008;61:344-9.

RESEARCH ARTICLE

DOI: 10.4274/AdvRadiolImaging.galenos.2026.21931
Adv Radiol Imaging 2026;3(2):32-37

Incidental Degenerative Lumbar Disc Findings in Pediatric Patients: A Retrospective MRI Study Using the Pfirrmann Classification

Özlem Çelik Aydın[1], Hatice Kübra Özdemir[2], Habibe Eser[2]

[1]*Erzincan Binali Yıldırım University Faculty of Medicine, Department of Radiology, Erzincan, Türkiye*
[2]*University of Health Sciences Türkiye, Ankara Etlik City Hospital, Clinic of Radiology, Ankara, Türkiye*

Abstract

Objectives: Degenerative intervertebral disc findings are well recognized in adults, but remain less clearly defined in pediatric patients, particularly when incidentally detected on magnetic resonance imaging (MRI). This study aimed to evaluate the prevalence, severity, and anatomical distribution of incidental degenerative lumbar disc findings in pediatric patients undergoing MRI for indications unrelated to degenerative spinal disease.

Methods: This retrospective observational study included 73 pediatric patients who underwent abdominal, pelvic, or lumbar MRI examinations with adequate visualization of the lumbar spine. Patients with known spinal trauma, previous spinal surgery, congenital spinal malformation, infection, malignancy, inflammatory spondyloarthropathy, or whose MRI was performed primarily for suspected degenerative spinal disease were excluded. Intervertebral discs were evaluated on sagittal T2-weighted images according to the Pfirrmann classification. Disc-level distribution, number of affected discs, Modic-type endplate changes, disc bulging, protrusion, and extrusion, and demographic variables were recorded.

Results: The study population consisted of 33 males (45.2%) and 40 females (54.8%), with a mean age of 11.8±4.2 years. Fifty-two patients (71.2%) had Pfirrmann grade 1 discs. Pfirrmann grade 2 and grade 3 degeneration were detected in 12 patients (16.4%) and 9 patients (12.3%), respectively. Overall, Pfirrmann grade 2 or higher disc degeneration was observed in 21 patients (28.8%). No Pfirrmann grade 4 or 5 degeneration was identified. Degenerative disc findings increased with age and were most frequent in the 13-17-year age group. No patient aged 6 years or younger showed disc degeneration. The affected levels were predominantly located in the lower lumbar spine, especially at L4-L5 and L5-S1. No marked sex-related differences were observed.

Conclusion: Incidental degenerative lumbar disc findings may be detected in pediatric patients, particularly during adolescence. These findings are usually low-grade, are limited to Pfirrmann grade 2 or 3 changes, and predominantly involve the lower lumbar levels. Awareness of this imaging spectrum may help radiologists avoid both underrecognition and overinterpretation of incidental degenerative disc findings in pediatric MRI.

Keywords: Pediatric MRI, lumbar spine, incidental findings, Pfirrmann classification, disc degeneration, intervertebral disc

Introduction

Magnetic resonance imaging (MRI) is widely used in the pediatric population because of its high soft-tissue contrast, multiplanar capability, and lack of ionizing radiation. Although spinal MRI is most commonly requested for specific clinical conditions such as low back pain, neurological deficits, trauma, scoliosis, infection, or suspected congenital abnormalities, the lumbar spine may also be partially or completely visualized during abdominal and pelvic MRI examinations performed for non-spinal indications. This has increased the detection of incidental vertebral and intervertebral disc abnormalities in children and adolescents.

Degenerative changes of the intervertebral discs and adjacent vertebral endplates are well-recognized findings in adults and are frequently detected even in asymptomatic individuals.[1,2] In the adult population, disc desiccation, disc height reduction, bulging, protrusion, annular fissures, and Modic endplate changes are common MRI findings, and their prevalence generally increases with age.[3-5] However, the presence and clinical significance of similar findings in pediatric patients remain less clearly defined. Because degenerative spinal disease is

Cite this article as: Çelik Aydın Ö, Özdemir HK, Eser H. Incidental degenerative lumbar disc findings in pediatric patients: a retrospective MRI study using the Pfirrmann classification. Adv Radiol Imaging. 2026;3(2):32-37

Address for Correspondence: Habibe Eser MD, University of Health Sciences Türkiye, Ankara Etlik City Hospital, Clinic of Radiology, Ankara, Türkiye
E-mail: habibeserr@gmail.com **ORCID ID:** orcid.org/0009-0000-4175-5715
Received: 06.07.2026 **Accepted:** 13.08.2026 **Published:** 31.08.2026

traditionally considered uncommon in children, these abnormalities may be overlooked or interpreted inconsistently when encountered incidentally.

Previous pediatric and adolescent MRI studies have shown that degenerative disc findings are not completely absent in younger age groups.[6-8] Low-grade disc signal alterations, early Pfirrmann grade changes, mild disc bulging, and rare Modic-type vertebral endplate signal abnormalities have been reported, particularly in older adolescents.[8,9] The lower lumbar levels, especially L4-L5 and L5-S1, appear more frequently involved, which may reflect the greater biomechanical load and mobility in these segments. Nevertheless, the reported prevalence varies considerably among studies because of differences in patient selection, imaging indication, age distribution, symptomatic status, and classification methods.

Standardized radiological classification systems are important for evaluating these findings objectively. The Pfirrmann grading system provides a reproducible method for assessing intervertebral disc degeneration based on disc signal intensity, disc structure, distinction between the nucleus pulposus and annulus fibrosus, and disc height.[10,11] Similarly, Modic classification allows systematic evaluation of vertebral endplate and adjacent bone marrow signal changes.[3,4] Using such grading systems in pediatric cohorts may help distinguish minimal age-related or developmental alterations from potentially relevant early degenerative pathology.

Despite the increasing use of MRI in children, limited information remains on the frequency and distribution of incidental degenerative vertebral and disc findings in pediatric patients undergoing MRI for indications unrelated to degenerative spinal disease. Most available data are derived either from symptomatic adolescents with low back pain or from asymptomatic adult populations. Therefore, evaluating pediatric patients who were scanned for indications that were neither spinal nor degenerative may provide a clearer estimate of the incidental burden of early degenerative spinal findings.

The aim of the present study was to assess the prevalence, severity, and anatomical distribution of incidental degenerative intervertebral disc and vertebral endplate findings in pediatric patients undergoing MRI for indications other than degenerative spinal disease. Particular attention was given to Pfirrmann grade distribution, number of affected disc levels, involved lumbar segments, Modic-type vertebral marrow changes, and associated findings such as disc bulging or herniation. This approach may improve awareness of early degenerative spinal findings in pediatric MRI and contribute to more accurate radiological reporting.

Methods

Study Design and Patient Population

This retrospective observational study included pediatric patients who underwent abdominal, pelvic, or lumbar magnetic resonance imaging examinations for indications unrelated to degenerative spinal disease. Ethical approval was granted by the Clinical Research Ethics CommiVee at Erzincan Binali Yıldırım University (approval no: 78924, date: 25.06.2026). Institutional approval was obtained before data collection, and the requirement for written informed consent was waived because of the retrospective nature of the study.

A total of 73 pediatric patients were included in the final analysis. Patients were eligible for inclusion if their MRI examinations adequately demonstrated the lumbar vertebrae and intervertebral disc levels from the upper lumbar region to the lumbosacral junction. Patients who underwent MRI primarily for suspected degenerative spinal disease, known spinal trauma, previous spinal surgery, congenital spinal malformation, spinal infection, malignancy, inflammatory spondyloarthropathy, or inadequate image quality were excluded from the study.

Demographic data, including age and sex, were obtained from the hospital information system. The clinical indication for MRI was also documented when available. Since the aim of the study was to evaluate incidental degenerative vertebral and disc findings, only patients without a primary clinical suspicion of degenerative lumbar spine pathology were included.

MRI Protocol

All MRI examinations were performed using a 1.5-T MRI scanner with standard body or spine coils, according to clinical indication. The imaging protocol varied slightly depending on whether the examination was performed for abdominal, pelvic, or spinal indications; however, only examinations that provided sufficient visualization of the lumbar vertebral column and intervertebral discs were included.

Sagittal T2-weighted images were used as the primary sequence for evaluating intervertebral disc signal intensity, disc height, disc morphology, and Pfirrmann grade. Sagittal T1-weighted images were evaluated for vertebral marrow signal characteristics and endplate-related changes. Axial T2-weighted images, when available, were used to confirm disc contour abnormalities such as bulging, protrusion, extrusion, or canal compromise. Fat-suppressed T2-weighted or STIR images were used to support the assessment of vertebral endplate edema or inflammatory-like marrow signal alterations when present.

Image Analysis

All MRI examinations were retrospectively reviewed by radiologists experienced in musculoskeletal and abdominal imaging. The readers evaluated the lumbar intervertebral discs and adjacent vertebral endplates by consensus. The following parameters were recorded: presence and grade of disc degeneration, number of affected disc levels, anatomical distribution of affected levels, presence of Modic-type endplate changes, disc bulging, disc protrusion, disc extrusion, disc height loss, and vertebral marrow or endplate abnormalities.

Each lumbar intervertebral disc was evaluated separately. Disc degeneration was graded according to the Pfirrmann classification on sagittal T2-weighted images.[10] In this grading system, grade 1 represents a normal disc with a homogeneous hyperintense signal, normal disc height, and a clear distinction between the nucleus pulposus and the annulus fibrosus. Grade 2 indicates preserved disc height with an inhomogeneous but still hyperintense signal. Grade 3 is characterized by inhomogeneous, intermediate or gray signal intensity and an unclear distinction between the nucleus and annulus, with disc height normal or only mildly decreased. Grade 4 represents advanced signal loss, characterized by hypointense disc signal, loss of distinction between the nucleus and annulus, and mild-to- moderate disc height reduction. Grade 5 indicates severe disc degeneration, with marked loss of disc height and a collapsed, hypointense disc.

For each patient, the highest Pfirrmann grade and the total number of affected disc levels were recorded. Discs classified as Pfirrmann grade 2 or higher were considered to show degenerative signal alteration.

Pfirrmann grades 4 and 5 were specifically recorded when present because these grades represent more advanced degeneration.

Vertebral endplate and adjacent bone marrow changes were assessed according to the Modic classification.[3,4]. Modic type 1 change was defined as low signal intensity on T1-weighted images and high signal intensity on T2-weighted or fat-suppressed images, compatible with edema-like inflammatory marrow change. Modic type 2 change is defined as high signal intensity on T1-weighted images and iso- to hyperintense signal on T2-weighted images, reflecting fatty marrow replacement. Modic type 3 change was defined as low signal intensity on both T1- and T2-weighted images, consistent with subchondral sclerosis.[5] The presence, type, and affected vertebral level of Modic changes were recorded.

Disc bulging was defined as a generalized extension of disc tissue beyond the margins of the vertebral body, involving a broad portion of the disc circumference. Disc protrusion was defined as focal or broad-based displacement of disc material in which the base of the displaced disc material was wider than its outward extension. Disc extrusion was defined as focal disc displacement in which the outward extension of the herniated material exceeded the width of its base. Sequestration was defined as displaced disc material with no continuity with the parent disc. Annular fissure, when visible as a focal high-intensity zone within the posterior annulus on T2-weighted images, was also recorded.

The anatomical level of each degenerative disc finding was categorized as L1-L2, L2-L3, L3-L4, L4-L5, or L5-S1. The distribution of affected levels was analyzed separately for Pfirrmann grade 2 and Pfirrmann grade 3 degeneration. Particular attention was given to lower lumbar levels because previous pediatric and adolescent MRI studies have suggested that early degenerative changes are more frequently observed at L4-L5 and L5-S1.[6,8]

Statistical Analysis

Statistical analysis was performed using standard statistical software. Continuous variables were expressed as mean ± standard deviation or median with range, depending on distribution characteristics. Categorical variables were summarized as frequencies and percentages. The prevalence of Pfirrmann grade 2 and grade 3 disc degeneration, Modic changes, disc bulging, protrusion, extrusion, and other vertebral or disc abnormalities was calculated as a proportion of the total number of patients.

The distribution of degenerative findings by sex and age group was evaluated when appropriate. Comparisons between categorical variables were performed using the chi-square test or Fisher's exact test. Continuous variables were compared using the independent samples t-test or Mann-Whitney U test, depending on the normality of their distributions. A p value of less than 0.05 was considered statistically significant.

Results

Demographic Characteristics of the Study Population

A total of 73 pediatric patients were included in the study. Of these, 33 patients were male (45.2%) and 40 were female (54.8%). The mean age of the study population was 11.8±4.2 years, with an age range of 3 to 17 years.

When patients were categorized according to age groups, 11 (15.1%) were 6 years of age or younger, 27 (37.0%) were between 7 and 12 years of age, and 35 (47.9%) were between 13 and 17 years of age. Degenerative disc findings were observed more frequently among adolescents. No patient aged 6 years or younger had Pfirrmann grade 2 or grade 3 disc degeneration (Figures 1-4).

Age and Sex Distribution According to Pfirrmann Grade

Fifty-two patients (71.2%) had Pfirrmann grade 1 discs and were considered to have no degenerative disc signal alteration. Pfirrmann grade 2 disc degeneration was detected in 12 patients (16.4%), and grade 3 in 9 patients (12.3%). No patient had Pfirrmann grade 4 or 5 degeneration.

Patients with Pfirrmann grade 2 or 3 degeneration were older than those with Pfirrmann grade 1 discs. The mean age was 10.6±4.1 years in patients with Pfirrmann grade 1 discs, 13.7±2.1 years in patients with Pfirrmann grade 2 degeneration, and 15.2±1.4 years in patients with Pfirrmann grade 3 degeneration. Degenerative findings were predominantly observed in patients aged 13-17 years.

No marked sex predominance was observed among patients with degenerative disc findings. Pfirrmann grade 2 degeneration was observed in 5 males and 7 females, while Pfirrmann grade 3 degeneration was observed in 4 males and 5 females.

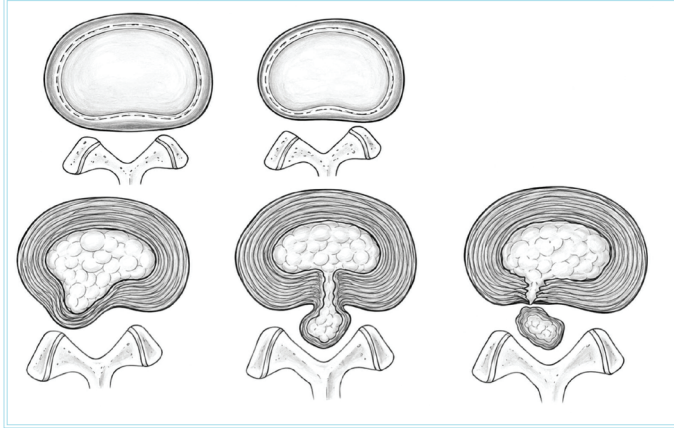

Figure 1. Schematic illustration of the Pfirrmann classification

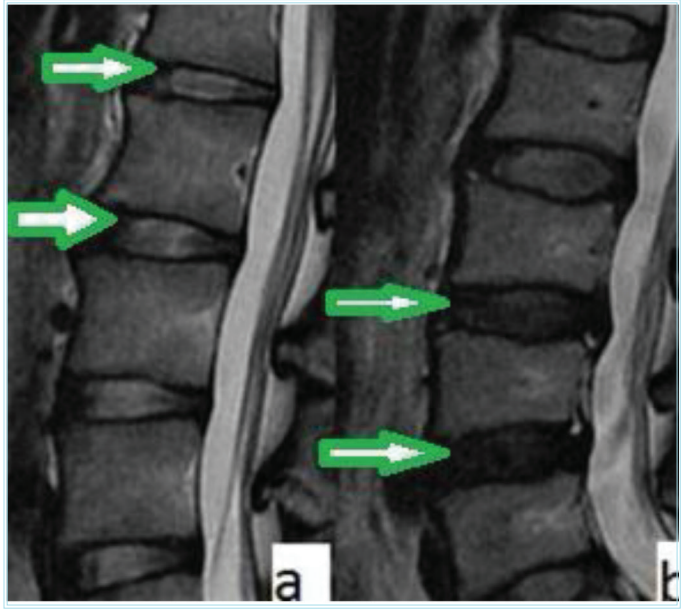

Figure 2. Pfirrmann grade 2 (**a**) and grade 3 (**b**) discs are shown (arrows)

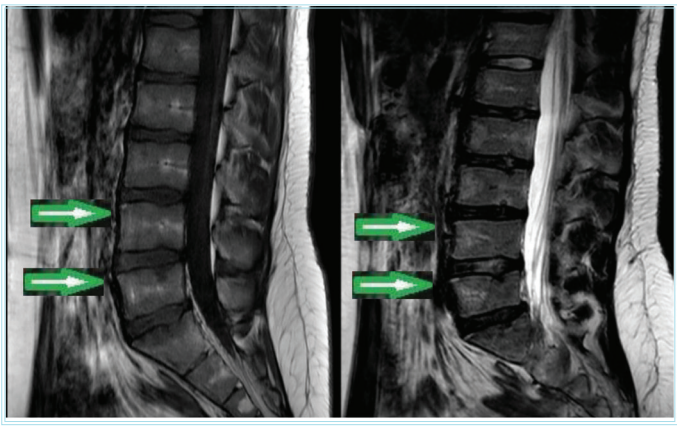

Figure 3. Modic type 2 degeneration is shown on sagittal T1-weighted and T2-weighted images, respectively

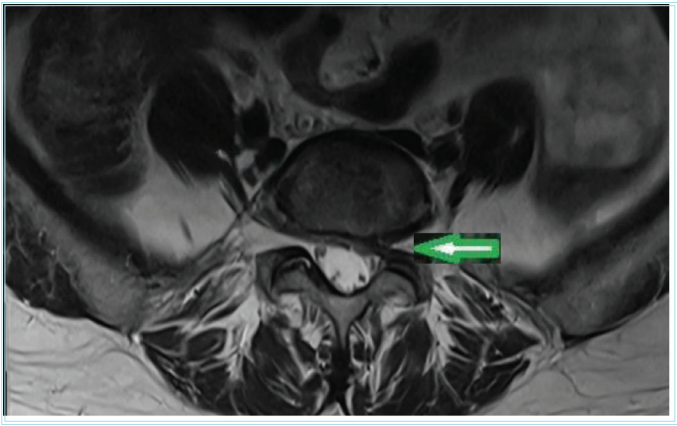

Figure 4. Disc bulging is shown on the T2-weighted

Overall, disc degeneration of Pfirrmann grade 2 or higher was detected in 21 of 73 patients (28.8%). The frequency and severity of disc degeneration increased with age. While no degenerative disc signal alteration was observed in children aged 6 years or younger, 5 of 27 patients (18.5%) in the 7-12-year age group and 16 of 35 patients (45.7%) in the 13-17-year age group demonstrated Pfirrmann grade 2 or 3 degeneration, respectively.

Among patients with degenerative disc changes, Pfirrmann grade 2 degeneration was slightly more frequent than Pfirrmann grade 3 degeneration. The distribution of degenerative changes did not show a clear sex-related difference. The affected disc levels and the number of involved discs are summarized separately for Pfirrmann grade 2 and grade 3 degeneration in Tables 1-4.

Among 73 pediatric patients, Pfirrmann grade 2 degeneration was detected in 12 patients (16.4%), and grade 3 in 9 patients (12.3%). No Pfirrmann grade 4 or 5 degeneration was identified. Degenerative disc findings were predominantly located in the lower lumbar spine, especially at L4-L5 and L5-S1.

Discussion

Incidental degenerative intervertebral disc findings were detected in 21 of 73 pediatric patients, corresponding to an overall prevalence of 28.8%. Pfirrmann grade 2 and grade 3 degeneration were observed in 12 patients (16.4%) and 9 patients (12.3%), respectively. No patient had Pfirrmann grade 4 or 5 disc degeneration. These findings indicate that degenerative disc signal alterations may be encountered in the pediatric population, although they are generally low-grade and rarely progress to advanced morphologic degeneration during childhood or adolescence.

Table 1. Demographic characteristics of the study population

Variable	n	%
Total number of patients	**73**	**100**
Sex		
Male	33	45.2
Female	40	54.8
Age group		
≤6 years	11	15.1
7-12 years	27	37.0
13-17 years	35	47.9
Age, years		
Mean ± SD	11.8±4.2	-
Range	3-17	-

SD: Standard deviation

Table 2. Distribution of Pfirrmann grades according to age and sex

Variable	Pfirrmann grade 1 n=52	Pfirrmann grade 2 n=12	Pfirrmann grade 3 n=9	Total n=73
Sex				
Male	24	5	4	33
Female	28	7	5	40
Age group				
≤6 years	11	0	0	11
7-12 years	22	4	1	27
13-17 years	19	8	8	35
Age, years				
Mean ± SD	10.6±4.1	13.7±2.1	15.2±1.4	11.8±4.2

SD: Standard deviation

Table 3. Distribution of patients with Pfirrmann grade 2 disc degeneration

Parameter	n	%
Number of affected discs per patient		
1 affected disc	9	12.3
2 affected discs	3	4.1
Total patients with Pfirrmann grade 2 degeneration	**12**	**16.4**
Affected disc level distribution		
L2-L3	1	1.4
L3-L4	2	2.7
L4-L5	6	8.2
L5-S1	6	8.2

Pfirrmann grade 2 degeneration was present in 12 of 73 patients (16.4%). The total number of affected disc levels was 15 because three patients had involvement at two levels

Table 4. Distribution of patients with Pfirrmann grade 3 disc degeneration

Parameter	n	%
Number of affected discs per patient		
1 affected disc	6	8.2
2 affected discs	2	2.7
3 affected discs	1	1.4
Total patients with Pfirrmann grade 3 degeneration	**9**	**12.3**
Affected disc level distribution		
L2-L3	1	1.4
L3-L4	2	2.7
L4-L5	5	6.8
L5-S1	5	6.8

Pfirrmann grade 3 degeneration was present in 9 of 73 patients (12.3%). The total number of affected disc levels was 13 because two patients had two-level involvement, and one patient had three-level involvement

The overall frequency of degenerative disc findings in our cohort is broadly consistent with previous pediatric MRI studies reporting that early degenerative spinal changes are not exceptional in children and adolescents, particularly when MRI examinations are reviewed systematically.[6-8] In the original study on which the present design was based, degenerative vertebral or disc-related findings were reported in approximately one-third of pediatric patients who underwent MRI for indications unrelated to degenerative spinal disease.[12] Similarly, previous studies have shown that low-grade disc signal changes, mild disc bulging, and vertebral endplate abnormalities may be incidentally detected in pediatric patients, although the reported prevalence varies according to age distribution, imaging indication, and diagnostic criteria.[7,9]

A noteworthy finding of the present study was the clear age-related distribution of degenerative changes. No patients aged 6 years or younger had Pfirrmann grade 2 or 3 degeneration, whereas degenerative disc changes were detected in 5 of 27 patients (18.5%) in the 7-12-year age group and 16 of 35 patients (45.7%) in the 13-17-year age group. This supports the concept that disc degeneration in pediatric patients is strongly age-dependent and becomes more apparent during adolescence.[6,7] The higher frequency in older children may reflect increasing axial load, greater spinal mobility, sports-related microtrauma, body growth, and progressive biochemical changes in the intervertebral disc matrix.[13]

The predominance of mild degeneration is another important finding. In our cohort, all degenerative discs were classified as Pfirrmann grades 2 or 3, and no advanced grades were observed. This pattern suggests that pediatric degenerative disc disease usually represents an early-stage imaging phenomenon rather than advanced structural failure. Pfirrmann grade 2 changes mainly reflect an inhomogeneous but still hyperintense disc signal with preserved disc height, whereas grade 3 changes indicate a more evident signal alteration with an unclear nucleus-annulus distinction but without marked disc collapse. Therefore, the absence of Pfirrmann grade 4 and 5 degeneration is compatible with the expected natural history of disc degeneration in a young population.

The anatomical distribution of affected disc levels also showed a consistent pattern. Both Pfirrmann grade 2 and grade 3 degenerative changes were more commonly observed at the lower lumbar levels, particularly L4-L5 and L5-S1. In the Pfirrmann grade 2 group, the most frequently affected levels were L4-L5 and L5-S1; each was involved in 6 disc levels. A similar pattern was observed in the Pfirrmann grade-3 group in which L4-L5 and L5-S1 were again the dominant levels. This lower lumbar predominance is biologically plausible because these segments are exposed to greater mechanical stress, higher mobility, and increased shear forces compared with upper lumbar levels. Similar lower lumbar clustering has also been emphasized in previous pediatric and adolescent MRI studies.[6,8,13,14]

In contrast to adult populations, in whom disc degeneration, disc height loss, bulging, protrusion, and Modic endplate changes are frequently encountered even in asymptomatic individuals, pediatric patients generally show fewer and milder degenerative abnormalities.[1,2] Adult MRI studies have demonstrated that degenerative findings increase substantially with age and may be present in a large proportion of individuals without back pain.[1,2] This creates an important interpretative issue: the presence of a degenerative imaging finding does not necessarily imply clinical relevance. The same principle should be applied carefully in pediatric imaging. Incidental low-grade Pfirrmann changes should be reported, but they should not be overinterpreted in the absence of concordant symptoms or other clinically significant abnormalities.

The lack of a marked sex-related difference in the present cohort is also consistent with the view that early pediatric disc degeneration is more closely related to age and segmental mechanical factors than to sex. Pfirrmann grade 2 degeneration was observed in 5 males and 7 females, while grade 3 degeneration was observed in 4 males and 5 females. Although the number of patients with degeneration was limited, these findings do not suggest a meaningful predominance of either males or females. Larger studies with balanced age and activity profiles would be required to determine whether sex, body mass index, physical activity, or sports participation modify the risk of early disc degeneration in pediatric patients.

The clinical significance of incidental degenerative disc changes in children remains uncertain. In symptomatic adolescents, disc degeneration and herniation may be associated with low back pain; however, in patients undergoing abdominal or pelvic MRI, or MRI for non-degenerative indications, these findings may simply reflect early structural adaptation or subclinical degeneration. Since the present study focused on incidental findings, radiological interpretation should be approached with caution. Low-grade Pfirrmann changes, particularly when isolated and unaccompanied by nerve root compression, marked disc height loss, or inflammatory endplate changes, may not require direct clinical intervention. Nevertheless, recognizing and documenting these findings may be useful for follow-up, especially in older adolescents or patients who later develop back pain.

Compared with the original 31-patient study, the present redesigned cohort preserves the same general radiological pattern but provides a broader sample size.[12] The original study reported Pfirrmann grades 2 and 3 degeneration in similar proportions and found no Pfirrmann grade 4 or 5 degeneration. In our expanded 73-patient dataset, the prevalences of Pfirrmann grades 2 and 3 degeneration remained comparable, and the overall rate of degenerative findings was 28.8%. This supports the internal consistency of the revised results and suggests that the new dataset remains compatible with the expected pediatric MRI spectrum.

Study Limitations

This study has several limitations. First, the retrospective design limits the ability to correlate imaging findings with detailed clinical symptoms, physical activity, body mass index, or longitudinal outcomes. Second, MRI protocols were not completely uniform because examinations were obtained for different clinical indications. Third, although the sample size was larger than that of the original study, subgroup analyses according to age, sex, and disc level remain limited by the relatively small number of patients with degenerative changes. Finally, because the study evaluated incidental findings, the true natural history and clinical consequences of these early disc abnormalities cannot be determined from these data.

Conclusion

Incidental degenerative disc findings can be detected in pediatric patients, particularly during adolescence. In the present cohort, these findings were predominantly low-grade, limited to Pfirrmann grades 2 and 3, and most frequently involved the lower lumbar levels, especially L4-L5 and L5S1. Advanced disc degeneration was not observed. These results support the view that early degenerative disc signal alterations are uncommon in younger children but become more visible in adolescents. Awareness of this imaging spectrum may help radiologists report pediatric lumbar MRI findings more accurately and avoid both underrecognition and overinterpretation of incidental degenerative changes.

Ethics

Ethics Committee Approval: Ethical approval was granted by the Clinical Research Ethics CommiVee at Erzincan Binali Yıldırım University (approval no: 78924, date: 25.06.2026).

Informed Consent: Due to the retrospective nature of the study, the requirement for written informed consent has been waived.

Footnotes

Authorship Contributions

Concept: Ö.Ç.A., Design: Ö.Ç.A., H.K.Ö., Data Collection or Processing: H.K.Ö., Analysis or Interpretation: H.E., Literature Search: Ö.Ç.A., H.E., Writing: Ö.Ç.A., H.K.Ö., H.E.

Conflict of Interest: No conflict of interest was declared by the authors.

Financial Disclosure: The authors declared that this study received no financial support.

References

1. Boden SD, Davis DO, Dina TS, Patronas NJ, Wiesel SW. Abnormal magnetic-resonance scans of the lumbar spine in asymptomatic subjects. A prospective investigation. J Bone Joint Surg Am. 1990;72:403-8.
2. Jensen MC, Brant-Zawadzki MN, Obuchowski N, Modic MT, Malkasian D, Ross JS. Magnetic resonance imaging of the lumbar spine in people without back pain. N Engl J Med. 1994;331:69-73.
3. Modic MT, Steinberg PM, Ross JS, Masaryk TJ, Carter JR. Degenerative disk disease: assessment of changes in vertebral body marrow with MR imaging. Radiology. 1988;166:193-9.
4. Modic MT, Masaryk TJ, Ross JS, Carter JR. Imaging of degenerative disk disease. Radiology. 1988;168:177-86.
5. de Roos A, Kressel H, Spritzer C, Dalinka M. MR imaging of marrow changes adjacent to end plates in degenerative lumbar disk disease. AJR Am J Roentgenol. 1987;149:531-4.
6. Kjaer P, Leboeuf-Yde C, Sorensen JS, Bendix T. An epidemiologic study of MRI and low back pain in 13-year-old children. Spine (Phila Pa 1976). 2005;30:798-806.
7. Urrutia J, Zamora T, Prada C. The prevalence of degenerative or incidental findings in the lumbar spine of pediatric patients: a study using magnetic resonance imaging as a screening tool. Eur Spine J. 2016;25:596-601.
8. Wan ZY, Zhang J, Shan H, Liu TF, Song F, Samartzis D, Wang HQ. Epidemiology of lumbar degenerative phenotypes of children and adolescents: a large-scale ımaging study. Global Spine J. 2023;13:599-608.
9. Ramadorai U, Hire J, DeVine JG, Brodt ED, Dettori JR. Incidental findings on magnetic resonance imaging of the spine in the asymptomatic pediatric population: a systematic review. Evid Based Spine Care J. 2014;5:95-100.
10. Pfirrmann CW, Metzdorf A, Zanetti M, Hodler J, Boos N. Magnetic resonance classification of lumbar intervertebral disc degeneration. Spine (Phila Pa 1976). 200126:1873-8.
11. Griffith JF, Wang YX, Antonio GE, et al. Modified Pfirrmann grading system for lumbar intervertebral disc degeneration. Spine (Phila Pa 1976). 2007;32:E708-12.
12. Gökharman FD, Aydın S, Kazcı Ö, Koşar PN. Incidental MRI findings for degenerative disc and vertebra pathologies in pediatric patients. Kırıkkale Uni Med J. 2018;20:26-32.
13. Yoshimizu R, Nakase J, Yoshioka K, et al. Incidence and temporal changes in lumbar degeneration and low back pain in child and adolescent weightlifters: a prospective 5-year cohort study. PLoS One. 2022;17:e0270046.
14. Modic MT, Steinberg PM, Ross JS, Masaryk TJ, Carter JR. Degenerative disk disease: assessment of changes in vertebral body marrow with MR imaging. Radiology. 1988;166:193-9.

RESEARCH ARTICLE

DOI: 10.4274/AdvRadiolImaging.galenos.2026.03511
Adv Radiol Imaging 2026;3(2):38-43

Radiologic Anatomy of the Tracheobronchial Tree: CT Morphometric Analysis of Branching Angle

Koray Bingöl, Hatice Çakır

Erzincan Binali Yıldırım University Faculty of Medicine, Department of Anatomy, Erzincan, Türkiye

Abstract

Objectives: To characterize the radiologic anatomy of tracheobronchial branching using computed tomography (CT)-based morphometric analysis and to evaluate the associations between branching angles and demographic variables, particularly age and sex, in pediatric and adult populations.

Methods: This retrospective cross-sectional study included 712 individuals (310 pediatric and 402 adults) who underwent thoracic CT. Four tracheobronchial angles were measured on coronal 25-mm minimum intensity projection images: the right-left main bronchial angle, right upper lobe bronchus-bronchus intermedius angle, right middle lobe bronchus-right lower lobe bronchus angle, and left upper lobe bronchus-left lower lobe bronchus angle. Angle measurements were compared according to age group and sex, and correlations with age were assessed.

Results: The mean right-left main bronchial angle was 70.1±13.1°. The right middle-lower bronchial angle was significantly greater in adults than in children (44.1±12.8° vs. 38.4±12.7°, p<0.001). In children, the right-left main angle was greater in boys than in girls (71.2±12.3° vs. 68.0±13.3°, p=0.029), whereas in adults it was greater in women than in men (72.4±14.0° vs. 68.7±12.3°, p=0.005). Age showed weak correlations with the right upper-intermedius angle (r=-0.102, p=0.006) and right middle-lower angle (r=0.159, p<0.001).

Conclusion: CT-based morphometric evaluation demonstrated that tracheobronchial branching geometry exhibits branch-specific anatomical variation associated with age and sex. Although the main bronchial bifurcation angle remained relatively stable across pediatric and adult populations, distal branching angles showed significant demographic differences. These findings provide radiologic anatomical reference data that may facilitate individualized interpretation of thoracic CT examinations and contribute to the anatomical assessment of patients undergoing bronchoscopic and thoracic procedures.

Keywords: Anatomic variation, morphometry, bronchi, tomography, X-ray computed

Introduction

The tracheobronchial tree is a complex three-dimensional anatomical system whose dimensions, branching angles, and spatial orientation exhibit considerable interindividual variability. Rather than representing a geometrically uniform conduit, central airway anatomy is influenced by demographic and anatomical factors, including age and sex, and may display substantial variation even among otherwise healthy individuals. Accurate characterization of this variability has important implications for diagnostic bronchoscopy, airway stenting, endotracheal and double-lumen tube placement, thoracic surgery, and patient-specific assessment of airflow and inhaled particle deposition. Advances in multidetector computed tomography (CT), multiplanar reconstruction, minimum intensity projection (MinIP), and three-dimensional post-processing now enable non-invasive and reproducible assessment of tracheobronchial morphology beyond the limitations of conventional radiography or cadaveric measurements.[1-3]

Historically, morphometric investigations have focused predominantly on the carinal, subcarinal, and interbronchial angles. However, published findings regarding the effects of age and sex have been inconsistent. Karabulut demonstrated sex-related differences in tracheal carinal geometry on CT, whereas subsequent large-scale CT studies reported population-dependent variation in bronchial dimensions and branching patterns.[2-4] In a multidetector CT study including pediatric and adult participants, Ulusoy et al.[3] showed that several tracheal and bronchial morphometric parameters varied by age and sex, supporting the concept that fixed reference values may inadequately represent the full spectrum of normal airway anatomy. Pediatric three-dimensional CT studies have likewise demonstrated age-related variability in tracheobronchial angulation, further indicating that airway geometry changes across the lifespan.[5] Differences in study populations, measurement definitions, respiratory phase, image reconstruction techniques, and two-dimensional versus three-dimensional assessment may partly explain the heterogeneity of reported results.

Cite this article as: Bingöl K, Çakır H. Radiologic anatomy of the tracheobronchial tree: CT morphometric analysis of branching angle. Adv Radiol Imaging. Adv Radiol Imaging. 2026;3(2):38-43

Address for Correspondence: Asst. Prof. Hatice Çakır, Erzincan Binali Yıldırım University Faculty of Medicine, Department of Anatomy, Erzincan, Türkiye
E-mail: dr.haticecakir24@gmail.com **ORCID ID:** orcid.org/0009-0009-5135-6561
Received: 08.07.2026 **Accepted:** 13.08.2026 **Published:** 31.08.2026

More recent studies have expanded the analysis beyond a single carinal or subcarinal angle. Using three-dimensional CT reconstruction, Erkaya et al.[6] evaluated multiple central and lobar bronchial branching angles and demonstrated complex associations with age, sex, and ipsilateral lung volume. Importantly, in a previous large-scale study by Kahraman et al.[7] —which comprised an independent patient population distinct from the present cohort— 1,511 pediatric and adult patients were evaluated using multislice CT and the MinIP technique. That study measured not only the right-left main bronchial angle but also the angles between the right upper lobe bronchus and the bronchus intermedius, between the right middle lobe bronchus and the right lower lobe bronchus, and between the left upper lobe bronchus and the left lower lobe bronchus. It reported a mean tracheal bifurcation angle of 73.3°±13.7° and demonstrated age- and sex-related differences in selected branching angles, thereby substantially expanding available CT-based reference data across a broad age range. Nevertheless, subsequent three-dimensional evidence suggests that tracheobronchial geometry may reflect a more complex interaction among demographic characteristics, lung morphology, and branch-specific spatial relationships than a single bifurcation measurement can capture.

The clinical relevance of such anatomical variability has become increasingly apparent. A recent randomized controlled trial demonstrated that individualized rotation of a left-sided double-lumen tube based on the left main bronchial angle measured on preoperative CT increased the first-attempt placement success rate from 82.6% to 91.4% and reduced procedure-related morbidity.[8] Similarly, three-dimensional reconstruction studies have shown that demographic characteristics and conventional two-dimensional radiographic estimates may not adequately account for individual variation in bronchial size when selecting double-lumen tubes.[9] These findings emphasize that precise CT-based characterization of airway geometry is not merely descriptive but may contribute directly to personalized procedural planning and to safer airway management.

Despite these advances, substantial heterogeneity persists across studies with respect to angular definitions, reconstruction techniques, age distribution, and anatomical levels assessed, limiting the generalizability of, and direct comparisons between, available reference data. Therefore, the present study aimed to comprehensively characterize tracheobronchial branching geometry using CT-based measurements and to evaluate its associations with demographic variables, particularly age and sex. Although our research group has previously investigated tracheobronchial branching angles across a large-scale pediatric and adult cohort utilizing the MinIP technique, the present study builds upon that foundational work by providing a more refined morphological assessment, exploring detailed age- and sex-stratified reference parameters, and offering a deeper anatomical analysis of tracheobronchial geometry across distinct demographic groups. By providing branch-specific morphometric data, this study seeks to refine normative anatomical reference values and strengthen the basis for individualized radiological, bronchoscopic, anesthetic, and thoracic surgical applications.

Methods

Study Design and Population

This retrospective study was conducted after approval by the Institutional Review Board (approval number: 2026-15/05, date: 06.08.2026). Owing to the retrospective nature of the investigation, the requirement for written informed consent was waived by the ethics committee. Thoracic CT examinations retrieved between January 2023 and January 2026 were evaluated. Thoracic CT examinations were performed for various clinical indications, primarily for trauma evaluation, suspected pulmonary infection, persistent cough, and exclusion of metastasis.

The study cohort comprised 712 patients, including 310 pediatric and 402 adult participants. Participants were classified into a pediatric group (age range: 1-18 years; mean: 13.7±4.5 years) and an adult group (age range: 19-92 years; mean: 55.6±18.1 years).

Of 855 initially screened thoracic CT examinations, patients were excluded due to respiratory motion, artifactual images, inability to comply with breath-hold instructions, insufficient breath-holding resulting in inadequate image quality, or acquisition during the expiratory phase (n=31). Additional exclusion criteria included a history of tracheobronchial or lung surgery (n=23); tracheal intubation; traumatic pneumothorax (n=25) or pneumomediastinum (n=26); and conditions capable of altering mediastinal anatomy, including mediastinal masses, mediastinal lymphadenopathy, and severe cardiomegaly (n=29). Individuals with related musculoskeletal deformities, such as kyphoscoliosis (n=9), were also excluded from the study based on these predefined criteria. As a result, the final analyzed patient group consisted of 712 individuals.

CT Acquisition and Image Analysis

Both contrast-enhanced and non-contrast thoracic CT examinations were included. Both contrast-enhanced and non-contrast CT examinations were evaluated together without a prior separate comparison, because intravenous contrast administration does not substantially alter the geometric or angular relationships of the cartilaginous tracheobronchial tree. Imaging was performed using a dual-source 256-slice CT scanner (Somatom Definition Flash; Siemens Healthcare, Forchheim, Germany). Both pediatric and adult examinations followed standardized institutional scanning protocols, with tube voltage and current parameters adjusted according to patient age and body habitus. All examinations were retrieved from the Picture Archiving and Communication System and reviewed on a Siemens workstation using Syngo.Via software, with particular emphasis on coronal reconstructions and MinIP images.

The CT acquisition protocol included a tube voltage of 120 kV, automatic tube current modulation ranging from 100 to 250 mAs, a section thickness of 1.25 mm, a pitch of 1.4, a gantry rotation time of 0.5-1 s, and a field of view of 455 mm. Examinations were obtained with patients in the supine position and, whenever possible, during adequate inspiration. For contrast-enhanced thoracic CT, 100-120 mL of iodinated contrast material was administered intravenously at an injection rate of 4 mL/s.

Image measurements were subsequently performed on coronal reconstructions generated with a 25-mm MinIP slab using Syngo.via software (Siemens Healthineers, Erlangen, Germany). Two radiologists independently performed the measurements, after which the findings were reviewed by an additional radiologist. Any disagreement between readers was resolved through joint reassessment and consensus. The investigators remained unaware of the patients' ages during the measurement process until the completion of the image analysis. Complete blinding to sex and clinical information was not feasible because anatomical features, including skeletal maturity, could provide indirect visual cues.

Patient age and sex were recorded as demographic variables. All angular measurements were obtained from coronal lung-window MinIP images. The following tracheobronchial branching angles were assessed:

- The angle between the right and left main bronchi;

- The angle between the right upper lobe bronchus and bronchus intermedius;

- The angle between the right middle lobe bronchus and right lower lobe bronchus;

- The angle between the left upper lobe bronchus and left lower lobe bronchus.

For each measurement, reference lines were drawn along the central longitudinal axes of the relevant bronchi, and the angle at their intersection was recorded (Figure 1). The central longitudinal axes were manually defined through the center of the air-filled bronchial lumen on standardized coronal multiplanar reformations, while the MinIP slab orientation was kept fixed at 25 mm.

MinIP is a post-processing technique designed to enhance visualization of low-attenuation structures. Within a predefined volume, the algorithm selects the voxel with the lowest attenuation value along each viewing direction and projects these data onto a two-dimensional image. This approach is particularly suitable for depicting air-filled structures such as the tracheobronchial tree.

For consistency, the measured parameters were designated as follows: the right main bronchus-left main bronchus angle was termed the right-left main coronal angle; the right upper lobe bronchus-bronchus intermedius angle was termed the right upper-intermedius coronal angle; the right middle lobe bronchus-right lower lobe bronchus angle was termed the right middle-lower coronal angle; and the left upper lobe bronchus-left lower lobe bronchus angle was termed the left upper-lower coronal angle.

Statistical Analysis

Statistical analyses were performed using IBM SPSS Statistics for Windows, version 20.0 (IBM Corp., Armonk, NY, USA). The distributions of continuous variables were assessed using the Kolmogorov-Smirnov test. Normally distributed numerical data were summarized as mean ± standard deviation, whereas variables with non-normal distributions were reported as median (minimum-maximum). Categorical variables were presented as frequencies and percentages.

Depending on the data distribution, comparisons of continuous variables between groups were conducted using either the Student's t-test or the Mann-Whitney U test. Categorical variables were compared using the chi-square test or Fisher's exact test, as appropriate. Associations between age and tracheobronchial angular measurements were examined using Spearman correlation analysis. Because multiple subgroup comparisons were performed across age categories and sex, these analyses were considered exploratory, and marginal significance levels (such as p=0.029) were interpreted with appropriate caution. A two-sided p value of <0.05 was considered statistically significant.

Results

The study population comprised 712 patients, including 310 pediatric patients (43.5%) and 402 adults (56.5%). The mean age was 13.7±4.5 years in the pediatric group and 55.6±18.1 years in the adult group, with an overall mean age of 37.4±25.0 years. Sex distribution was comparable between the pediatric and adult groups (p=0.713).

No significant differences were observed between pediatric and adult patients in the right-left main coronal angle, right upper-intermedius coronal angle, or left upper-lower coronal angle. In contrast, the right middle-lower coronal angle was significantly smaller in the pediatric group than in the adult group (38.4±12.7° vs. 44.1±12.8°, p<0.001) (Table 1).

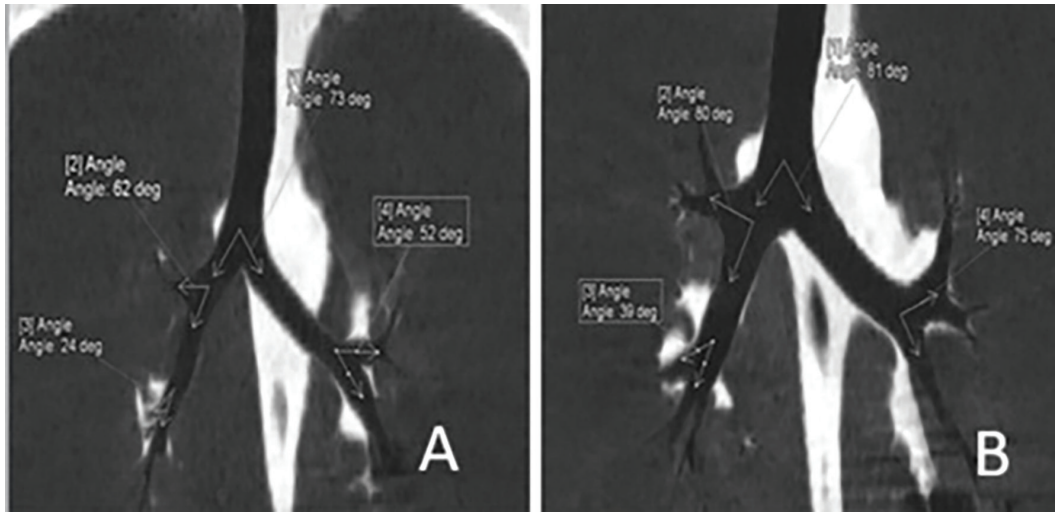

Figure 1. Measurement of tracheobronchial branching angles on coronal thoracic images obtained using the MinIP technique in pediatric and adult patients. A) Measurements in a 9-year-old boy. B) Measurements in a 25-year-old man. The assessed angles were as follows: (1) the angle between the right and left main bronchi in the coronal plane; (2) the right upper-intermedius angle, formed by the right upper lobe bronchus and bronchus intermedius; (3) the right middle-lower angle, formed by the right middle lobe bronchus and right lower lobe bronchus; and (4) the left upper-lower angle, formed by the left upper lobe bronchus and left lower lobe bronchus

MinIP: Minimum intensity projection

Within the pediatric group, the right-left main coronal angle was significantly greater in boys than in girls (71.2±12.3° vs. 68.0±13.3°, p=0.029). No significant sex-related differences were detected in the right upper-intermedius, right middle-lower, or left upper-lower coronal angles. In the adult group, the right-left main coronal angle was significantly smaller in men than in women (68.7±12.3° vs. 72.4±14.0°, p=0.005), whereas the remaining branching angles did not differ significantly according to sex (Table 2).

Correlation analysis demonstrated a significant negative association between age and the right upper-intermedius coronal angle (r=-0.102, p=0.006), and a significant positive association between age and the right middle-lower coronal angle (r=0.159, p<0.001). The correlations between age and the right-left main coronal angle (r=0.067, p=0.074) and between age and the left upper-lower coronal angle (r=-0.073, p=0.052) did not reach statistical significance (Table 3).

Table 3. Relationship between age and angles

Variables (coronal; angles in°)	r	p
Right-left main	0.067	0.074
R upper-intermedius	-0.102	0.006
R middle-lower	0.159	<0.001
L upper-lower	-0.073	0.052

R upper-intermedius: angle between the right upper lobe bronchus and bronchus intermedius in the coronal plane; R middle-lower: angle between the right middle lobe bronchus and right lower lobe bronchus in the coronal plane; L upper-lower: angle between the left upper lobe bronchus and left lower lobe bronchus in the coronal plane

Discussion

The principal findings of the present study were as follows: first, the overall right-left main coronal angle was 70.1±13.1°, with no significant difference between pediatric and adult patients. Second, the right middle-lower coronal angle was significantly greater in adults than in pediatric patients (44.1±12.8° vs. 38.4±12.7°, p<0.001). Third, sex-related differences in the right-left main coronal angle showed an age-dependent pattern: in the pediatric group, the angle was greater in boys than in girls, whereas in the adult group it was smaller in men than in women. Finally, increasing age was associated with a modest decrease in the right upper-intermedius coronal angle and an increase in the right middle-lower coronal angle, while correlations with the right-left main coronal and left upper-lower coronal angles did not reach statistical significance. Taken together, these findings indicate that tracheobronchial geometry is not uniform across the airway tree and that demographic effects may vary according to both the anatomical level assessed and the age group under consideration.

The mean right-left main coronal angle observed in the present cohort was broadly consistent with the range reported in previous CT-based morphometric investigations. Karabulut reported mean interbronchial and subcarinal angles of approximately 77° and 73°, respectively, and demonstrated a strong relationship between the two measurement approaches.[4] Kamel et al.,[10] using both *in vivo* CT and cadaveric assessment, also emphasized the marked interindividual variability of subcarinal geometry, reporting a wide range of values and no consistent association with age or sex. Similarly, large-scale CT analyses have demonstrated considerable variability in central airway dimensions and branching morphology across individuals.[2] Such differences between studies are likely to reflect, at least in part, heterogeneity in patient characteristics, respiratory phase, anatomical landmarks, and image-processing methodology.

A particularly relevant comparison is provided by our previous study, in which 1,511 pediatric and adult patients were evaluated using

Table 1. Demographic and clinical characteristics

Variables (coronal; angles in°)	Whole population, n=712	Pediatric group, n=310	Adult group, n=402	p
Age (year)	37.4±25.0	13.7±4.5	55.6±18.1	<0.001
Sex, n (%)				0.713
Male	357 (50.1)	153 (49.4)	204 (50.7)	
Female	355 (49.9)	157 (50.6)	198 (49.3)	
Right-left main	70.1±13.1	69.6±12.9	70.5±13.3	0.340
R upper-intermedius	72.1±13.4	72.9±12.9	71.6±13.8	0.193
R middle-lower	41.6±13.1	38.4±12.7	44.1±12.8	<0.001
L upper-lower	55.7±12.2	56.2±12.2	55.3±12.2	0.361

Numerical variables are expressed as mean ± standard deviation. A p value of was considered statistically significant. R upper-intermedius: angle between the right upper lobe bronchus and the bronchus intermedius in the coronal plane; R middle-lower: angle between the right middle lobe bronchus and the right lower lobe bronchus in the coronal plane; L upper-lower: angle between the left upper lobe bronchus and the left lower lobe bronchus in the coronal plane

Table 2. Distribution of demographic and clinical findings by sex

Variables (coronal; angles in°)	Pediatric male, n=153	Pediatric female, n=157	p	Adult male, n=204	Adult female, n=198	p
Age (year)	13.4±4.7	14.0±4.3	0.242	54.7±18.0	56.6±18.1	0.292
Right-left main	71.2±12.3	68.0±13.3	0.029	68.7±12.3	72.4±14.0	0.005
R upper-intermedius	72.0±12.4	73.7±13.3	0.245	71.8±13.6	71.3±14.0	0.717
R middle-lower	38.7±12.4	38.1±13.1	0.679	43.8±12.7	44.5±13.0	0.585
L upper-lower	56.1±12.7	56.2±11.8	0.943	55.7±11.3	54.9±13.1	0.513

Numerical variables are expressed as mean ± standard deviation. A p value <0.05 was considered statistically significant

multislice CT and the MinIP technique, yielding an overall tracheal bifurcation angle of 73.3±13.7°. The present findings reproduce this general pattern despite a lower absolute mean value, with pediatric and adult patients again showing comparable right-left main coronal measurements and demonstrating that the principal main-bronchial bifurcation angle remains relatively stable when comparing pediatric and adult populations at the group level.[7] At the same time, the modest difference in absolute values between cohorts reinforces the need to interpret reference ranges in relation to population structure and measurement conditions rather than consider a single universal threshold applicable to all individuals. The methodological framework and four branch-specific angular measurements in the previous study are documented in the initially uploaded article.[7]

In contrast to the relatively stable right-left main angle, the right middle-lower coronal angle demonstrated a clear difference among age groups. Adults had significantly larger values than pediatric patients; this parameter also showed the strongest positive correlation with age among all angular measurements. This finding closely parallels our previous study, in which the right middle-lower angle was likewise significantly greater in adults than in children.[7] The consistency of this branch-specific pattern with previous findings is noteworthy because most earlier studies concentrated on the carinal or subcarinal angle and provided limited information on more distal lobar branching geometry. More recent three-dimensional CT analyses have expanded this approach by demonstrating that bronchial branching angles differ according to anatomical level and may be related to demographic characteristics and lung morphology.[6] Therefore, the present data further support the concept that age-related remodeling of the tracheobronchial tree should be evaluated regionally rather than inferred from a single central bifurcation measurement.

The sex-related findings also warrant particular attention. In pediatric patients, boys had a significantly greater right-left main coronal angle than girls; the opposite pattern was observed in adults, with women showing larger angles than men. Although these independent subgroup comparisons revealed opposite descriptive patterns between pediatric and adult populations, formal interaction analysis was not performed. Therefore, these findings should be interpreted as distinct descriptive observations rather than definitive proof of an age-group-by-sex interaction. This finding closely mirrors the age-dependent sex pattern identified in our previous study.[7] Earlier investigations have produced inconsistent results concerning sex-related variation in tracheobronchial angles. Karabulut[4] reported greater interbronchial and subcarinal angles in women, whereas Kamel et al.[10] found substantial variability without a significant sex relationship. Large-population CT studies have nevertheless confirmed that multiple tracheobronchial dimensions differ between men and women.[2,3] These discrepancies suggest that the influence of sex may not be constant throughout life and may depend on the specific airway parameter under investigation. The reversal of the male-female relationship between pediatric and adult groups in the present study may reflect differences in thoracic growth, lung volume development, body habitus, or age-related remodeling of mediastinal geometry; however, these mechanisms cannot be established from the present data and should be regarded as hypotheses requiring dedicated longitudinal investigation.

Previous pediatric studies further support the importance of considering developmental changes in airway geometry. Wani et al.[5] used three-dimensional CT-based measurements and showed that right and left bronchial angles in children vary with age, with particularly relevant developmental differences during early childhood. Herek et al.[11] likewise reported age-related changes in tracheobronchial angles in children, observing wider angles in younger age groups and a tendency for several central airway measurements to decrease with increasing age. In the present study, however, age was not significantly correlated with the right-left main coronal angle, whereas age showed a significant negative correlation with the right upper-intermedius angle and a significant positive correlation with the right middle-lower angle. The discrepancy is not necessarily contradictory; rather, it may indicate that maturation does not affect all bronchial branches in parallel. Differences in age ranges, sample compositions, two- versus three-dimensional assessments, and definitions of angular landmarks may contribute to heterogeneous findings across studies.

An additional observation is that the correlations with age were modest in magnitude. The strongest association was detected for the right middle-lower angle ($r=0.159$), while the right upper-intermedius angle showed only a weak inverse relationship ($r=-0.102$). Notably, our previous larger study identified statistically significant correlations between age and all four angular parameters, although the corresponding correlation coefficients were also small.[7] In the present cohort of 712 patients, the right-left main and the left upper-lower correlations did not achieve statistical significance. This difference may partly reflect the smaller sample size compared with that of the previous 1,511-patient cohort because the detection of very weak correlations is particularly sensitive to statistical power. More importantly, the consistently low magnitude of the correlation coefficients suggests that chronological age alone accounts for a limited proportion of interindividual variation in tracheobronchial geometry. This interpretation is compatible with three-dimensional morphometric work indicating that airway angles may be influenced by multiple interacting factors rather than by age alone.[6]

From an imaging perspective, the use of MinIP is an important feature of the present approach. MinIP preferentially displays low-attenuation voxels and therefore facilitates visualization of air-filled tracheobronchial structures. Our previous study demonstrated the feasibility of applying a 25-mm MinIP slab for branch-specific angular assessment in a large cohort of pediatric and adult participants.[7] Earlier MinIP-based investigations predominantly focused on the subcarinal angle,[12] whereas the present approach includes both central and lobar branching levels. Nevertheless, differences between MinIP, conventional multiplanar reconstructions, and three-dimensional airway segmentation should be acknowledged because each method may define the bronchial axis differently. The increasing use of three-dimensional CT reconstruction has demonstrated that airway geometry is inherently spatial and may not always be completely represented by a single coronal measurement.[5,6]

The clinical relevance of individualized tracheobronchial geometry extends beyond descriptive anatomy. Precise knowledge of bronchial orientation may facilitate bronchoscopy, airway reconstruction, lung isolation, and the selection or positioning of endobronchial devices. In particular, a recent randomized controlled trial demonstrated that individualizing left double-lumen tube rotation based on the left main bronchial angle measured on preoperative CT scans improved first-attempt placement success compared with conventional fixed rotation.[8] Likewise, three-dimensional reconstruction studies have shown that conventional demographic or two-dimensional approaches

may inadequately predict individual bronchial dimensions for double-lumen tube selection.[9] Earlier investigations demonstrated that direct CT measurement of the left main bronchus can guide individualized double-lumen tube sizing.[13,14] These observations support the broader premise that CT-derived airway morphometry can have procedural implications, although the current study was anatomical in nature and did not directly assess clinical outcomes.

Study Limitations

Several limitations should be acknowledged. First, the retrospective, single-center design may limit the generalizability of the findings. Second, although examinations with inadequate image quality and expiratory acquisition were excluded, subtle variability in inspiratory depth could still have influenced bronchial orientation. Third, measurements were obtained in the coronal plane using MinIP images, therefore, the full three-dimensional orientation of obliquely coursing bronchi may not have been fully represented. Fourth, although age and sex were analyzed, potentially relevant variables such as height, body mass index, thoracic dimensions, total lung volume, and pulmonary function parameters were unavailable for inclusion in multivariable models. Finally, the cross-sectional design does not permit direct evaluation of longitudinal changes in airway geometry within the same individuals. Future multicenter studies combining standardized inspiratory CT, automated airway segmentation, and three-dimensional morphometric analysis may help establish more robust population-specific reference ranges and clarify the independent determinants of branch-specific airway geometry.

Conclusion

The present study demonstrates that tracheobronchial branching geometry varies according to anatomical level and is differentially associated with age and sex. The right-left main coronal angle did not differ significantly between the pediatric and adult groups, whereas the right middle-lower angle was greater in adults and increased with age. Sex-related differences in the main bronchial angle exhibited opposite patterns between pediatric and adult populations, suggesting that demographic effects on airway morphology may be age-dependent. The close agreement of several key patterns with our previous large-scale MinIP study, particularly the greater right middle-lower angle in adults and the contrasting sex distribution of the right-left main angle, supports the consistency of these observations with our previous findings.[7] Further three-dimensional and longitudinal studies are warranted to determine the biological basis and procedural relevance of these branch-specific variations

Ethics

Ethics Committee Approval: This retrospective study was conducted after approval by the Institutional Review Board (approval number: 2026-15/05, date: 06.08.2026).

Informed Consent: This retrospective study.

Footnotes

Authorship Contributions

Concept: K.B., Design: K.B., Data Collection or Processing: K.B., Analysis or Interpretation: K.B., Literature Search: H.Ç., Writing: H.Ç.

Conflict of Interest: No conflict of interest was declared by the authors.

Financial Disclosure: The authors declared that this study received no financial support.

References

1. Christou S, Chatziathanasiou T, Angeli S, et al. Anatomical variability in the upper tracheobronchial tree: sex-based differences and implications for personalized inhalation therapies. J Appl Physiol (1985). 2021;130:678-707.
2. Mi W, Zhang C, Wang H, et al. Measurement and analysis of the tracheobronchial tree in Chinese population using computed tomography. PLoS One. 2015;10:e0123177.
3. Ulusoy M, Uysal II, Kıvrak AS, et al. Age and gender related changes in bronchial tree: a morphometric study with multidedector CT. Eur Rev Med Pharmacol Sci. 2016;20:3351-7.
4. Karabulut N. CT assessment of tracheal carinal angle and its determinants. Br J Radiol. 2005;78:787-90.
5. Wani TM, Buchh B, AlGhamdi FS, Jan R, Tumin D, Tobias JD. Tracheobronchial angles in children: Three-dimensional computed tomography-based measurements. Paediatr Anaesth. 2018;28:463-7.
6. Erkaya A, Coskun ZK, Akyol S, et al. Evaluation of angles of the tracheobronchial tree with the 3-dimensional reconstruction method: a morphometric and radiologic study. Int J Morphol. 2023;41:512-7.
7. Kahraman Ş, Yazar MF, Aydemir H, Kantarci M, Aydin S. Detection of tracheal branching with computerized tomography: the relationship between the angles and age-gender. World J Radiol. 2023;15:118-26.
8. Zhou H, Fei Y, Zhang Y, Quan X, Yi J. Individualized rotation of left double lumen endobronchial tube to improve placement success rate: a randomized controlled trial. Respir Res. 2024;25:184.
9. Mihatsch LL, Weiland S, Helmberger T, Friederich P. Common double-lumen tube selection methods overestimate adequate tube sizes in individual patients - a 3D reconstruction study. BMC Anesthesiol. 2024;24:215.
10. Kamel KS, Lau G, Stringer MD. In vivo and in vitro morphometry of the human trachea. Clin Anat. 2009;22:571-9.
11. Herek D, Herek O, Ufuk F. Tracheobronchial angle measurements in children: an anthropometric retrospective study with multislice computed tomography. Clin Exp Otorhinolaryngol. 2017;10:188-92.
12. Fernandes SF, Pradhan A. Estimation of subcarinal angle using minimum intensity projection in computed tomography. Asian J Pharm Clin Res. 2018;11:383-5.
13. Hannallah M, Benumof JL, Silverman PM, Kelly LC, Lea D. Evaluation of an approach to choosing a left double-lumen tube size based on chest computed tomographic scan measurement of left mainstem bronchial diameter. J Cardiothorac Vasc Anesth. 1997;11:168-71.
14. Chow MY, Liam BL, Lew TW, Chelliah RY, Ong BC. Predicting the size of a double-lumen endobronchial tube based on tracheal diameter. Anesth Analg. 1998;87:158-60.

RESEARCH ARTICLE

DOI: 10.4274/AdvRadiolImaging.galenos.2026.43153
Adv Radiol Imaging 2026;3(2):44-49

Impact of Ureteral Stone Size and Location on Hydronephrosis Severity: A Retrospective Non-contrast CT Study

Muhammet Fırat Öztepe, Ali Osman Gülmez

Erzincan Binali Yıldırım University Faculty of Medicine, Department of Radiology, Erzincan, Türkiye

Abstract

Objectives: To evaluate the relationship between stone size, stone location, and the presence and severity of hydronephrosis in patients with a single unilateral ureteral stone identified on non-contrast computed tomography (CT).

Methods: In this retrospective single-center study, adult patients with a single, unilateral ureteral stone detected on non-contrast CT examinations of the urinary tract performed between February 7, 2022, and April 13, 2026, were included. Stone size, location, hydronephrosis status and grade, and accompanying imaging findings were recorded. Associations between stone characteristics and hydronephrosis severity were assessed using correlation analyses, chi-square tests, and regression models. Receiver operating characteristic (ROC) analysis was performed to evaluate the ability of stone size to predict moderate-to-severe hydronephrosis.

Results: A total of 128 patients were included. The median age was 45 years; 77.3% were male. Hydronephrosis was present in 116 patients (90.6%), while 58 patients (45.3%) had moderate-to-severe hydronephrosis. Stone size increased significantly with greater hydronephrosis severity (rho=0.422, p<0.001). In multivariable ordinal logistic regression analysis, each 1-mm increase in stone size was independently associated with a higher hydronephrosis grade [odds ratio (OR): 1.20, 95% confidence interval (CI): 1.07-1.33, p=0.001]. Proximal or mid-ureteral stones were also independently associated with greater hydronephrosis severity compared with distal/ureterovesical junction stones (OR: 2.40, 95% CI: 1.14-5.07, p=0.022). The area under the curve for predicting moderate-to-severe hydronephrosis was 0.747.

Conclusion: Increasing stone size is independently associated with greater hydronephrosis severity in patients with a single unilateral ureteral stone. Proximal or mid-ureteral stone locations are also associated with more advanced hydronephrosis. These findings suggest that stone characteristics may provide valuable information regarding the severity of urinary tract obstruction.

Keywords: Ureteral stone, hydronephrosis, computed tomography, urinary obstruction

Introduction

Ureteral stones are a common cause of acute flank pain and can lead to urinary obstruction ranging from mild collecting system dilation to significant hydronephrosis requiring urgent treatment. Non-contrast computed tomography (CT) is a fundamental confirmatory imaging modality in patients with suspected acute ureteral stone because it accurately demonstrates the presence, size, and location of the stone and permits evaluation of accompanying urinary system dilation. These findings are clinically important because the likelihood of ongoing obstruction and spontaneous stone passage is low, which are key factors influencing the decision for active treatment.[1,2]

Stone size and location are well-known determinants of the likelihood of spontaneous passage. Small and distally located ureteral stones are more likely to pass spontaneously, while intervention is more frequently reported for large and proximally located stones.[3,4] Hydronephrosis, as an imaging finding of obstruction, can provide additional information to the clinical evaluation. In a large multicenter cohort including patients with confirmed ureteral stones via CT, it was reported that the frequency of stones of 5 mm and above and the rate of spontaneous passage failure increased with increasing severity of hydronephrosis.[5]

However, the number of studies directly evaluating the relationship between the size and localization of ureteral stones and the degree of hydronephrosis is limited. Song et al.[6] reported that in patients with a single unilateral ureteral stone, stone diameter was associated with the degree of hydronephrosis, but stone localization did not show a significant relationship. A study from Türkiye also showed that an increase in stone size was associated with a higher degree of hydronephrosis, while there was no significant relationship between

Cite this article as: Öztepe MF, Gülmez AO. Impact of ureteral stone size and location on hydronephrosis severity: a retrospective non-contrast CT study. Adv Radiol Imaging. 2026;3(2):44-49

Address for Correspondence: Ali Osman Gülmez MD, Erzincan Binali Yıldırım University Faculty of Medicine, Department of Radiology, Erzincan, Türkiye
E-mail: aliosmangulmez.2@gmail.com ORCID ID: orcid.org/0000-0001-7050-1765
Received: 25.06.2026 Accepted: 09.08.2026 Published: 31.08.2026

stone localization and the degree of hydronephrosis.[7] In a more recent study, all urinary system stones were evaluated and it was reported that larger stones were associated with more advanced degrees of hydronephrosis; however, this study was not limited to ureteral stones only.[8]

The aim of this retrospective study was to evaluate the relationship between stone size and localization, and the presence and degree of hydronephrosis in patients with unilateral single ureteral stones identified on non-contrast CT scans.

Methods

Study Design and Patient Selection

The study was approved by the Erzincan Binali Yıldırım University Non-Interventional Clinical Research Ethics Committee (approval no: 2026-01/03; date: 08.01.2026). The requirement for informed consent from the ethics committee was waived. Non-contrast urinary system CT reports in our institution's radiology report archive, issued between February 7, 2022, and April 13, 2026, were searched using keywords related to ureteral stones. A total of 150 cases with reported ureteral stones were included in the initial dataset.

The study included adult patients whose non-contrast CT report clearly indicated a single unilateral ureteral stone, with stone size reported in millimeters and the presence and degree of hydronephrosis documented. Patients with bilateral ureteral stones, those with multiple ureteral stones on the same examination, and those with poor image quality were excluded. Based on these criteria, the main analysis cohort consisted of 128 patients.

Data Collection and Variable Definition

Information on patients' ages, gender, stone side, stone localization, stone size, presence and degree of hydronephrosis, concomitant renal stones, and contamination of the perirenal and periureteral fatty planes was extracted.

Stone localization was classified into three groups: proximal ureter, mid ureter, and distal ureter/ureterovesical junction (UVJ). Stones described as at the ureteropelvic junction or in the proximal ureter were evaluated in the proximal group; stones described as at the UVJ or in the distal ureter were evaluated in the distal/UVJ group. Stone size was recorded as a continuous variable in millimeters; it was also divided into three categories: <5 mm, 5-<10 mm, and ≥10 mm, similar to classifications in previous studies.[6,7] Hydronephrosis was graded on non-contrast CT according to the degree of dilatation of the renal collecting system and associated changes in the calyces and renal parenchyma. Hydronephrosis was classified into four categories: none, minimal/mild, moderate, and severe. No hydronephrosis was defined as the absence of dilatation of the collecting system. Minimal or mild hydronephrosis was defined as dilatation of the renal pelvis, calyces, or both with preservation of normal renal parenchymal thickness. Moderate hydronephrosis was defined as a more pronounced dilatation of the renal pelvis and calyces with calyceal rounding or increased calyceal prominence, without substantial renal parenchymal thinning. Severe hydronephrosis was defined as marked dilatation of the renal pelvis and calyces accompanied by renal parenchymal thinning. The grading approach was based on previously described imaging criteria for the assessment of hydronephrosis severity in patients with ureteral calculi.[8] Contamination of the perirenal and periureteral fatty planes was recorded.

Outcome Variables

The primary outcome of the study was the relationship of stone size and localization with the degree of hydronephrosis. In secondary analyses, hydronephrosis was classified as absent/minimal-mild and moderate/severe, the latter representing clinically more pronounced dilation. The predictive performance of stone size for moderate/severe hydronephrosis was also evaluated. The relationship between perirenal contamination and moderate/severe hydronephrosis was investigated in an exploratory analysis.

Statistical Analysis

The distribution of continuous variables was evaluated using visual and analytical methods. Continuous variables that were non-normally distributed were presented as median and interquartile range (IQR), and categorical variables as number and percentage. The Kruskal-Wallis test was used to compare stone size across hydronephrosis grades. The relationship between stone size and ordinal hydronephrosis grade was assessed using Spearman's rank correlation.

Relationships among stone size categories, stone localization, and the degree of hydronephrosis were examined using Pearson's chi-square test; p-values obtained using the Monte Carlo method were reported for comparisons in which the expected cell counts were low. In the multivariate logistic regression analysis, the presence of moderate/severe hydronephrosis was taken as the dependent variable, and stone size, stone localization, age, and gender were included as independent variables. In addition, an ordinal logistic regression was performed with the degree of hydronephrosis as the ordinal outcome.

The ability of stone size to differentiate moderate from severe hydronephrosis was evaluated using receiver operating characteristic analysis, and the area under the curve (AUC) was reported with its 95% confidence interval. The optimal threshold was determined in an exploratory manner using the Youden index. All tests were two-way, and $p<0.05$ was accepted as the level of statistical significance. Statistical analyses were performed using IBM SPSS Statistics for Windows, version 23.0 (IBM Corp., Armonk, NY, USA).

Findings

Initially, 150 patients with reported ureteral stones were identified. Of these, 5 patients were excluded because of bilateral ureteral stones, 8 because of multiple ureteral stones, 4 because the stone localization could not be assigned to a single ureteral segment, and 5 because of insufficient image quality. Thus, 128 patients were included in the final analysis.

The median age of the main cohort was 45.0 years (IQR, 37.0-56.2); 99 (77.3%) patients were male. 66 (51.6%) of the stones were located in the right ureter, and 62 (48.4%) were located in the left ureter. The median stone size was 6.0 mm (IQR, 4.0-8.5; range, 2.0-27.0 mm). 52 (40.6%) of the stones were located in the proximal ureter, 8 (6.2%) in the mid-ureter, and 68 (53.1%) in the distal ureter or at the UVJ. The median stone size was 6.0 mm (IQR, 4.5-9.0 mm) in the proximal ureter, 5.5 mm (IQR, 4.0-7.0 mm) in the mid-ureter, and 5.5 mm (IQR, 3.5-8.0 mm) in the distal ureter/UVJ. Hydronephrosis was present in 116 patients (90.6%), with moderate or severe hydronephrosis detected in 58 patients (45.3%) (Table 1, Figure 1).

Stone size increased with the severity of hydronephrosis. Median stone sizes were 5.0 mm (IQR, 4.0-6.0); 4.75 mm (IQR, 4.0-6.5); 6.5 mm (IQR, 5.5-10.0); and 9.0 mm (IQR, 7.0-9.93) in patients without hydronephrosis, with minimal or mild, moderate, and severe hydronephrosis, respectively. The difference between the groups was statistically significant (Kruskal-Wallis H=26.434; p<0.001). A moderate positive correlation was found between stone size and the degree of hydronephrosis (rho=0.422; p<0.001) (Table 2, Figure 2).

Table 1. Demographic and imaging characteristics of the main analysis cohort

Variable	Value
Total number of patients	128
Age, years; median (IQR)	45.0 (37.0-56.2)
Gender	
Male	99 (77.3)
Female	29 (22.7)
Stone side	
Right	66 (51.6)
Left	62 (48.4)
Stone size, mm; median (IQR)	6.0 (4.0-8.5)
Stone size, mm; range	2.0-27.0
Stone location	
Proximal ureter	52 (40.6)
Mid-ureter	8 (6.2)
Distal ureter/UVJ	68 (53.1)
Presence of hydronephrosis	
Absent	12 (9.4)
Present	116 (90.6)
Grade of hydronephrosis	
Absent	12 (9.4)
Minimal/mild	58 (45.3)
Moderate	48 (37.5)
Severe	10 (7.8)
Moderate/severe hydronephrosis	58 (45.3)
Concomitant renal stone	63 (49.2)
Perirenal/periureteral stranding	47 (36.7)

Categorical variables are presented as number and percentage
IQR, Interquartile range; UVJ, Ureterovesical junction

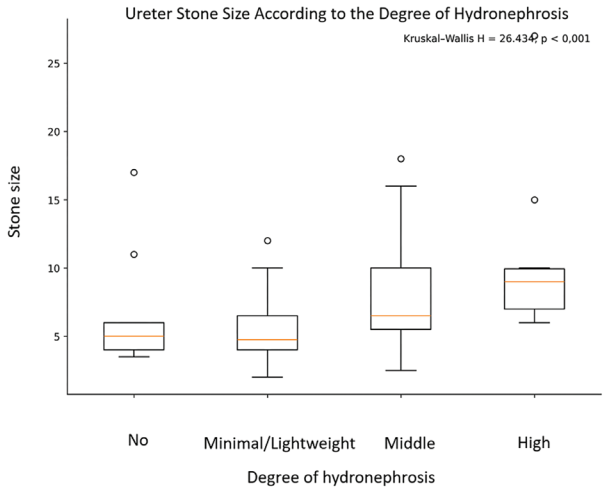

Figure 1. Ureter stone size according to degree of hydromephrosis

The rates of moderate-to-severe hydronephrosis differed significantly across stone size categories. Moderate/severe hydronephrosis was observed in nine patients (20.9%) with <5 mm stones, in 33 patients (51.6%) with 5-<10 mm stones, and in 16 patients (76.2%) with ≥10 mm stones (χ^2=21.755; Monte Carlo p<0.001) (Table 2).

Stone localization was also related to the degree of hydronephrosis. The rate of moderate/severe hydronephrosis was 61.5% (32/52) in patients with proximal ureteral stones, 75.0% (6/8) in mid-ureteral stones, and 29.4% (20/68) in distal/UVJ stones (χ^2=19.153; Monte Carlo p=0.005) (Table 3).

In multivariate ordinal logistic regression analysis, each 1 mm increase in stone size was associated with an increased probability of a higher degree of hydronephrosis (OR, 1.20; 95% CI: 1.07-1.33; p=0.001). Proximal- or middle-located stones were also independently associated with a higher degree of hydronephrosis compared with distal- or UVJ-located stones (OR, 2.40; 95% CI: 1.14-5.07; p=0.022). Age and gender were not significant independent predictors (Table 4).

In the logistic regression analysis, in which hydronephrosis was classified as absent/minimal-mild and moderate/severe, each 1-mm increase in stone size was associated with an increased probability of moderate/severe hydronephrosis (OR, 1.28; 95% CI: 1.09-1.50; p=0.002). Proximal or middle location was also associated with moderate to severe hydronephrosis (OR, 2.40; 95% CI: 1.06-5.45; p=0.036) (Table 4).

The ability of stone size to distinguish moderate from severe hydronephrosis was moderate (AUC, 0.747; 95% CI: 0.663-0.828). For the exploratory threshold of ≥5.2 mm, sensitivity was 82.8% and specificity was 61.4% (Table 4). This threshold was derived from the present dataset for exploratory purposes and should not be interpreted as a clinical decision threshold. No significant association was found between the presence of perirenal/periureteral contamination and moderate/severe hydronephrosis (p=0.417).

Discussion

In this study, the relationship between stone size and location and the degree of hydronephrosis was evaluated in patients with single unilateral ureteral stones identified on non-contrast CT scans. The main finding was that the degree of hydronephrosis increased significantly with stone size: each 1 mm increase in stone size was associated with a 20% increased probability of a higher degree of hydronephrosis (OR, 1.20; 95% CI: 1.07-1.33; p=0.001) and a 28% increased probability of moderate/severe hydronephrosis (OR, 1.28; 95% CI: 1.09-1.50; p=0.002). Furthermore, proximal- and middle-located stones were associated with a higher degree of hydronephrosis compared to distal/UVJ stones (OR, 2.40; 95% CI: 1.14-5.07; p=0.022).

The association between stone location and hydronephrosis severity persisted after adjustment for stone size, age, and gender in the multivariable ordinal logistic regression model. Proximal/middle ureteral location was associated with higher odds of having a greater hydronephrosis grade compared with the distal/UVJ location (OR, 2.40; 95% CI: 1.14-5.07; p=0.022), indicating that the observed association was not explained solely by stone size. One possible explanation is that the anatomical level of obstruction may influence the extent of

Table 2. Relationship between stone size and grade of hydronephrosis

A. Stone size according to grade of hydronephrosis

Grade of hydronephrosis	Number of patients	Stone size, mm; median (IQR)	Stone size, mm; mean ± SD
None	12	5.00 (4.00-6.00)	6.25±3.92
Minimal/mild	58	4.75 (4.00-6.50)	5.27±2.14
Moderate	48	6.50 (5.50-10.00)	7.95±3.88
Severe	10	9.00 (7.00-9.93)	10.67±6.28

A. Statistical analysis: Kruskal-Wallis H=26.434; p<0.001. Spearman correlation between stone size and grade of hydronephrosis: rho=0.422; p<0.001

B. Distribution of hydronephrosis according to stone size categories

Stone size category	Number of patients	No HN	Minimal/mild HN	Moderate HN	Severe HN	Moderate/severe HN, n (%)
<5 mm	43	5	29	9	0	9 (20.9)
5-<10 mm (51.6)	64	5	26	26	7	33
≥10 mm (76.2)	21	2	3	13	3	16

B. Statistical analysis: Monte Carlo Pearson chi-square test: χ^2=21.755; p<0.001

C. Pairwise comparison of stone size across hydronephrosis grades

Comparison	Adjusted p-value
None vs. minimal/mild	0.621
None vs. moderate	0.116
None vs. severe	0.024
Minimal/mild vs. moderate	<0.001
Minimal/mild vs. severe	<0.001
Moderate vs. severe	0.141

Holm correction was applied for pairwise comparisons
HN: Hydronephrosis, IQR: Interquartile range, SD: Standard deviation

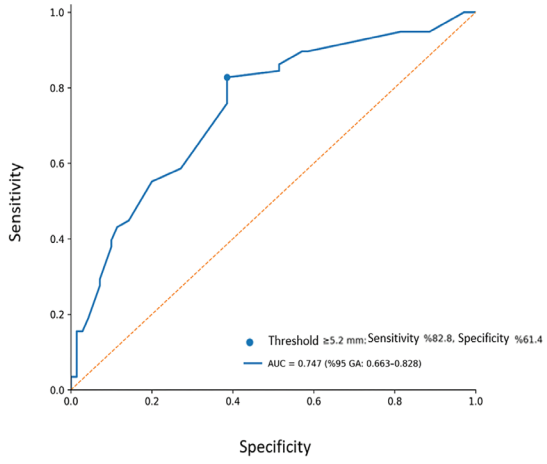

Figure 2. Performance of stone size in distinguishing moderate from severe hydronephrosis

AUC: Area under the curve

upstream urinary tract dilatation. However, this interpretation should be considered with caution because data on symptom duration, obstruction duration, and other clinical factors that may affect hydronephrosis were not available in our dataset. In addition, the small number of mid-ureteral stones limits the precision and generalizability of the localization findings.

The relationship between stone size and the degree of hydronephrosis is generally consistent with findings from previous studies. Song et al.[6] reported that stone diameter and craniocaudal stone length were significantly associated with the degree of hydronephrosis in 248 patients with unilateral single ureteral stones. Akçiçek and Buğday[7] from Türkiye also showed that the degree of hydronephrosis increased with increasing stone size in a cohort of 105 patients. Similarly, Alshoabi et al.[9] reported that larger stones were associated with higher-grade hydronephrosis; however, their study only evaluated stones causing hydronephrosis and included stones from the renal pelvis and pelviureteric junction. Our study evaluates this relationship in a more homogeneous clinical cohort, as it includes patients without hydronephrosis and focuses exclusively on solitary unilateral ureteral stones.

It has previously been shown that hydronephrosis is not merely a secondary diagnostic finding but may also be related to stone burden and the clinical course. Innes et al.[5] reported that in a large multicenter cohort with CT-confirmed ureteral stones, the frequency of stones larger than 5 mm and spontaneous passage failure increased with increasing severity of hydronephrosis. Goertz and Lotterman showed that the rate of stones larger than 5 mm was higher in patients with moderate/severe hydronephrosis compared to those with no/mild hydronephrosis.[10] Leo et al.[11] reported that the absence of hydronephrosis reduced the likelihood of larger ureteral stones and that stones larger than 5 mm may be associated with short-term clinical events. In our study, the AUC for stone size in differentiating moderate from severe hydronephrosis

Table 3. Relationship between stone location and grade of hydronephrosis

	Stone location	Number of patients no HN	Minimal/mild HN	Moderate HN	Severe HN	Moderate/severe HN, n (%)
Proximal ureter	52	2	18	28	4	32 (61.5)
Mid-ureter	8	0	2	4	2	6 (75.0)
Distal ureter/UVJ	68	10	38	16	4	20 (29.4)

Statistical analysis: Monte Carlo Pearson chi-square test: χ^2=19.153; p=0.005
Due to the low number of patients in the mid-ureter group, the rates for this group should be interpreted with caution
HN: Hydronephrosis, UVJ: Ureterovesical junction

Table 4. A. Multivariate analyses and ROC analysis for hydronephrosis grade and moderate/severe hydronephrosis

Variable	OR	95% CI	p value
Stone size, per 1 mm increase	1.20	1.07-1.33	0.001
Proximal/mid location vs. distal/UVJ	2.40	1.14-5.07	0.022
Age, per 1-year increase	1.00	0.98-1.03	0.677
Female vs. male	1.42	0.64-3.15	0.392
B. Binary logistic regression analysis for moderate/severe hydronephrosis			
Variable	**OR**	**95% CI**	**p value**
Stone size, per 1 mm increase	1.28	1.09-1.50	0.002
Proximal/mid location vs. distal/UVJ	2.40	1.06-5.45	0.036
Age, per 1-year increase	1.01	0.98-1.03	0.643
Female vs. male	1.74	0.68-4.46	0.252
C. Performance of stone size in discriminating moderate/severe hydronephrosis			
ROC analysis parameter	Result		
AUC	0.747		
95% CI	0.663-0.828		
Exploratory optimal cutoff value	≥5.2 mm		
Sensitivity	82.8%		
Specificity	61.4%		

In the ordinal logistic regression analysis, the outcome variable was hydronephrosis grade: 0=none, 1=minimal/mild, 2=moderate, 3=severe. In the binary logistic regression analysis, the outcome variable was defined as the presence of moderate/severe hydronephrosis. The threshold value in the ROC analysis is exploratory in nature
AUC: Area under the curve, CI: Confidence interval, OR: Odds ratio, ROC: Receiver operating characteristic, UVJ: Ureterovesical junction

was 0.747. In our study, the AUC value of stone size in differentiating moderate/severe hydronephrosis was 0.747. This level suggests that stone size carries significant information regarding the severity of hydronephrosis but is not sufficient alone for clinical decision-making. The exploratory threshold of ≥5.2 mm was derived from this dataset and should not be considered a validated clinical cut-off or used as an independent threshold for clinical decision-making. Further studies with larger and independent cohorts are needed to determine whether a clinically meaningful threshold can be established.

Our finding that proximal/middle-located stones are associated with more advanced hydronephrosis differs from the results of Song et al.[6] and Akçiçek and Buğday,[7] who showed no significant association in terms of stone localization. This difference may be attributable to variations in cohort size, the creation of localization categories, or the timing of patient presentation. Indeed, it has been shown that secondary findings of ureteral obstruction on CT are affected not only by stone characteristics but also by symptom duration; Varanelli et al.[12] reported that the frequency of hydronephrosis and other secondary findings increased as the duration of pain increased. Therefore, our finding regarding localization should be interpreted cautiously because information on clinical duration and symptom onset is not available.

The association between stone location and hydronephrosis severity persisted after adjustment for stone size, age, and gender in the multivariable ordinal logistic regression model. Proximal/middle ureteral location was associated with higher odds of a greater hydronephrosis grade compared with distal/UVJ location (OR, 2.40; 95% CI: 1.14-5.07; p=0.022), indicating that the observed association was not explained solely by stone size. One possible explanation is that the anatomical level of obstruction may influence the extent of upstream urinary tract dilatation. However, this interpretation should be considered cautiously because symptom duration, duration of obstruction, and other clinical factors that may affect hydronephrosis were not available in our dataset. In addition, the small number of mid-ureteral stones limits the precision and generalizability of the localization finding.

No significant association was found between perirenal/periureteral contamination and moderate/severe hydronephrosis. This finding can be explained by the fact that perirenal contamination can reflect not only

the severity of obstruction but also other factors, such as the duration of obstruction, pressure changes, and the local inflammatory response. Previous studies have also reported that the relationship between secondary CT findings and stone size or degree of hydronephrosis is variable.[12,13]

Study Limitations

This study has some limitations. First, the retrospective, single-center design is susceptible to selection bias. Second, clinical outcomes such as symptom duration, renal function, indicators of infection, treatments administered, and spontaneous stone passage were not available. Finally, the generalizability and robustness of the localization analysis are limited by the small number of patients with mid-ureteral stones (n=8). Therefore, the findings regarding mid-ureteral stone location should be interpreted cautiously and confirmed in larger cohorts with more balanced distributions of stone locations.

Conclusion

In patients with unilateral single ureteral stones, increased stone size was independently associated with a higher degree of hydronephrosis, specifically moderate/severe hydronephrosis. Proximal or mid-ureteral stone location was also associated with greater severity of hydronephrosis in our cohort; however, this finding should be interpreted cautiously, given the small number of mid-ureteral stones and the retrospective study design. These findings should be validated in larger, prospective cohorts incorporating clinical and laboratory data before their potential implications for clinical decision-making can be determined. Future studies may further clarify the contribution of hydronephrosis to clinical decision-making by combining stone size and degree of hydronephrosis with symptom duration, laboratory results, and treatment requirements.

Ethics

Ethics Committee Approval: The study was approved by the Erzincan Binali Yıldırım University Non-Interventional Clinical Research Ethics Committee (approval no: 2026-01/03; date: 08.01.2026).

Informed Consent: The requirement for informed consent from the ethics committee was waived.

Footnotes

Authorship Contributions

Surgical and Medical Practices: M.F.Ö., Concept: M.F.Ö., Design: M.F.Ö., A.O.G., Data Collection or Processing: BA.O.G., Analysis or Interpretation: A.O.G., Literature Search: M.F.Ö., Writing: M.F.Ö., A.O.G.

Conflict of Interest: No conflict of interest was declared by the authors.

Financial Disclosure: The authors declared that this study received no financial support.

References

1. Skolarikos A, Geraghty R, Somani B, et al. European association of urology guidelines on the diagnosis and treatment of urolithiasis. Eur Urol. 2025;88:64-75.
2. Türk C, Petřík A, Sarica K, et al. EAU guidelines on diagnosis and conservative management of urolithiasis. Eur Urol. 2016;69:468-74.
3. Coll DM, Varanelli MJ, Smith RC. Relationship of spontaneous passage of ureteral calculi to stone size and location as revealed by unenhanced helical CT. AJR Am J Roentgenol. 2002;178:101-3.
4. Jendeberg J, Geijer H, Alshamari M, Cierzniak B, Lidén M. Size matters: the width and location of a ureteral stone accurately predict the chance of spontaneous passage. Eur Radiol. 2017;27:4775-85.
5. Innes GD, Scheuermeyer FX, McRae AD, Teichman JMH, Lane DJ. Hydronephrosis severity clarifies prognosis and guides management for emergency department patients with acute ureteral colic. CJEM. 2021;23:687-95.
6. Song Y, Hernandez N, Gee MS, Noble VE, Eisner BH. Can ureteral stones cause pain without causing hydronephrosis? World J Urol. 2016;34:1285-8.
7. Akçiçek M, Buğday MS. The relationship between the size and localization of the ureteral stone and the degree of hydronephrosis. JHVS. 2023;11:1101-9.
8. Goertz JK, Lotterman S. Can the degree of hydronephrosis on ultrasound predict kidney stone size? Am J Emerg Med. 2010;28:813-6.
9. Alshoabi SA, Binnuhaid AA, Almohtadi AM, et al. Association between nephrolith size and location and grade of hydronephrosis. Life (Basel). 2025;15:321.
10. Goertz JK, Lotterman S. Can the degree of hydronephrosis on ultrasound predict kidney stone size? Am J Emerg Med. 2010;28:813-6.
11. Leo MM, Langlois BK, Pare JR, et al. Ultrasound vs. computed tomography for severity of hydronephrosis and its importance in renal colic. West J Emerg Med. 2017;18:559-68.
12. Varanelli MJ, Coll DM, Levine JA, Rosenfield AT, Smith RC. Relationship between duration of pain and secondary signs of obstruction of the urinary tract on unenhanced helical CT. AJR Am J Roentgenol. 2001;177:325-30.
13. Hiller N, Berkovitz N, Lubashevsky N, Salaima S, Simanovsky N. The relationship between ureteral stone characteristics and secondary signs in renal colic. Clin Imaging. 2012;36:768-72.

RESEARCH ARTICLE

DOI: 10.4274/AdvRadiolImaging.galenos.2026.22932
Adv Radiol Imaging 2026;3(2):50-57

Diagnostic Yield of Routine Imaging Follow-up after Normal Hip Ultrasonography in Children with a Family History of Developmental Dysplasia of the Hip

Orhan Avcı[1], Elanur Avcı[2], Bilgesu Arıkan Ergün[3]

[1]*Atatürk State Hospital, Clinic of Radiology, Zonguldak, Türkiye*
[2]*Acılık Family Health Center, Clinic of Family Medicine, Zonguldak, Türkiye*
[3]*Ankara Etlik City Hospital, Clinic of Radiology, Ankara, Türkiye*

Abstract

Objectives: Developmental dysplasia of the hip (DDH) is an important disorder in which delayed diagnosis may lead to persistent deformity, functional impairment, and premature osteoarthritis. Although a positive family history is a recognized risk factor and commonly prompts early ultrasonographic screening, the need for imaging follow-up after a normal initial ultrasound remains uncertain.

Methods: In this retrospective study, records of 842 children screened ultrasonographically for DDH were reviewed. Children with bilateral Graf type I hips, a positive family history of DDH, and at least one subsequent imaging examination were included. The final cohort comprised 243 children. Follow-up consisted of repeat ultrasonography or anteroposterior pelvic radiography. Radiographs were assessed using Hilgenreiner, Perkin, and Shenton lines and acetabular angle measurements.

Results: The mean age was 10.3 months, and 172 children (70.8%) were female. Eighty-nine patients underwent repeat ultrasonography, and none showed abnormal ultrasonographic or physical examination findings. The remaining 154 patients underwent follow-up pelvic radiography; the Shenton line was preserved and the upper femoral epiphysis remained within the expected inferomedial quadrant in all cases. The mean acetabular angle was 25.4±0.7°. In seven patients with serial radiographs, initially higher acetabular angles decreased to below 21°. Nine patients had multiple risk factors, with no significant difference in mean acetabular angle compared with the overall cohort.

Conclusion: A positive family history appears important for initial DDH risk stratification but, in isolation, may not justify repeated imaging after a normal early ultrasound. Selective, individualized follow-up may reduce unnecessary examinations, radiation exposure, and parental anxiety.

Keywords: Developmental dysplasia of the hip, family history, ultrasonography, pelvic radiography, follow-up imaging, acetabular angle

Introduction

Developmental dysplasia of the hip (DDH) encompasses a broad spectrum of abnormalities, ranging from mild acetabular dysplasia and transient instability to fixed subluxation or complete dislocation. Because the disorder may be clinically subtle during early infancy, delayed recognition can result in persistent biomechanical impairment, gait disturbance, chronic pain, premature osteoarthritis, and the need for complex reconstructive surgery later in life.[1,2] Nevertheless, the natural history of DDH is heterogeneous: some mild forms of neonatal instability or sonographic immaturity resolve spontaneously, whereas clinically relevant dysplasia may persist or become apparent later. This variability continues to complicate decisions regarding whom to image, when to image, and how long surveillance should be maintained.[1,2]

Physical examination remains the cornerstone of early detection, but imaging plays a critical complementary role when examination findings are equivocal or when recognized risk factors are present. Ultrasonography is particularly valuable during the first months of life, when the femoral head is predominantly cartilaginous, whereas anteroposterior (AP) pelvic radiography becomes increasingly informative with progressive ossification.[3] Despite decades of screening experience, the optimal screening strategy remains a matter of debate.

Cite this article as: Avcı O, Avcı E, Arıkan Ergün B. Diagnostic yield of routine imaging follow-up after normal hip ultrasonography in children with a family history of developmental dysplasia of the hip. Adv Radiol Imaging. 2026;3(2):50-57

Address for Correspondence: Orhan Avcı MD, Atatürk State Hospital, Clinic of Radiology, Zonguldak, Türkiye
E-mail: md_orhan@hotmail.com **ORCID ID:** orcid.org/0000-0003-1610-7745
Received: 17.07.2026 **Accepted:** 23.08.2026 **Published:** 31.08.2026

Universal ultrasonographic screening may increase early case detection but can also identify transient abnormalities and increase follow-up and treatment burden, whereas selective screening seeks to concentrate imaging on infants with abnormal physical findings or predefined risk factors.[2,4] Accordingly, contemporary practice generally favors an age-adapted and risk-based approach rather than indiscriminate repeated imaging.[1,3]

Among the established risk factors for DDH, breech presentation, female sex, and a positive family history are consistently emphasized, and meta-analytic evidence supports the association between family history and an increased probability of DDH.[5] However, the presence of a risk factor at the time of initial screening is not equivalent to evidence that the same factor should, by itself, mandate prolonged radiologic surveillance after a normal early examination. This distinction is particularly relevant for infants who have an isolated positive family history because clinical practice varies substantially after a normal screening ultrasound. In some centers, these infants undergo routine repeat ultrasonography or a pelvic radiograph after 4-6 months of age, whereas other pathways allow discharge from imaging follow-up when the initial clinical and sonographic assessment is normal.[3,6-8]

Several studies have, therefore, examined the diagnostic yield of secondary imaging in children with a family history of DDH. Arumilli et al.[6] and Osarumwense et al.[7] questioned the necessity of routine radiographic follow-up in infants with a positive family history after reassuring early assessment. Tafazal and Flowers[8] similarly evaluated whether an early normal ultrasound should routinely be followed by later pelvic radiography and found limited support for indiscriminate secondary imaging. In a two-center cohort of 205 children with a positive family history and normal initial ultrasonographic findings, Aydin and Fatihoglu[9] reported no late DDH on repeat ultrasonography or follow-up radiography, suggesting that family history alone may have limited value as an automatic indication for continued imaging after a normal screening study. Consistent with this broader evidence base, Price et al.[10] demonstrated a very low yield of abnormal radiographs after a normal initial ultrasound within a selective screening program.

Taken together, the available literature supports family history as a meaningful marker for initial risk stratification, but provides less consistent evidence that an isolated family history should trigger routine late imaging once early clinical and ultrasonographic findings are normal. This unresolved distinction has practical implications because unnecessary follow-up can increase healthcare utilization, expose infants to avoidable ionizing radiation when radiography is used, prolong surveillance, and amplify parental concern without a commensurate diagnostic benefit.[3,9] A more precise definition of which infants truly benefit from secondary imaging is, therefore, essential to balance prevention of missed late dysplasia against over-investigation. Further evidence, focused specifically on outcomes after normal early ultrasonography, is needed to refine risk-based follow-up pathways and reduce unwarranted variation in DDH screening practice.

Methods

Ethics Approval

Ethical approval for this study was obtained from the Erzincan Binali Yıldırım University Clinical Research Ethics Committee (approval no: EBYU-KAEK-2025-21/16, date: 27.11.2025).

Study Design and Participants

This retrospective study was conducted following approval by the relevant institutional ethics committee. The medical records and imaging data of 842 children who underwent ultrasonographic screening for DDH were retrospectively reviewed.

Children were eligible for inclusion if the initial hip ultrasonography demonstrated bilateral Graf type I morphology, there was a documented positive family history of DDH, and at least one subsequent imaging examination was available. Patients with ultrasonographic findings other than Graf type I hips, those without a documented positive family history of DDH, and those without follow-up imaging were excluded. After applying the predefined eligibility criteria, 243 children constituted the final study population.

Physical Examination

Clinical hip examinations were performed by family physicians and pediatricians as part of routine clinical assessment. The examination included assessment of hip stability using the Barlow and Ortolani maneuvers, and evaluation of asymmetry in the gluteal and thigh skin folds. Galeazzi sign, limitation of hip abduction, and limb-length discrepancy were not systematically documented in the available medical records and were therefore not included as predefined clinical assessment parameters in this retrospective analysis.

Ultrasonographic and Radiographic Equipment

Ultrasonographic examinations were performed using high-resolution ultrasound systems equipped with high-frequency linear transducers. Ultrasound systems included Samsung RS85 Prestige with an LA3-16A linear transducer (Samsung Medison Co., Ltd., Seoul, Republic of Korea), Mindray Resona R9 and Resona R7 with an LM16-4U linear transducer (Shenzhen Mindray Bio-Medical Electronics Co., Ltd., Shenzhen, China), Toshiba Aplio 300 with a PLT-805AT (12-6.2 MHz) linear transducer (Canon Medical Systems Corporation, Otawara, Japan), and GE Logiq Fortis R4 with an ML6-15-D linear transducer (GE HealthCare, Chicago, IL, USA).

Standardized AP pelvic radiographs were obtained using digital radiography systems equipped with automatic exposure control, including the DR-Rad X3-C and DR-Rad X4-C systems (DRGEM Corporation, Gwangmyeong-si, Republic of Korea) and the Jumong digital radiography system (SG HealthCare Co., Ltd., Goyang-si, Republic of Korea). All radiographic examinations were performed using a standardized pediatric low-dose imaging protocol in accordance with institutional imaging procedures to minimize radiation exposure while maintaining diagnostic image quality.

Ultrasonographic Evaluation

Hip ultrasonography was performed according to the standardized Graf method by two specialist radiologists, who had 5 and 7 years of radiology experience, respectively, and were working at two different institutions. The radiologists were not blinded to clinical information provided by referring clinicians, including documented DDH-related risk factors. Previous imaging findings were also available to the radiologists at the time of image interpretation. Examinations were performed with the infant positioned in the lateral decubitus position and the hip maintained in a neutral position. A high-frequency linear transducer

(7.5-12 MHz) was oriented to obtain the standard coronal Graf plane, with appropriate visualization of the straight iliac line, acetabular roof, bony acetabular rim, labrum, and femoral head.

The alpha (α) and beta (β) angles were assessed on technically adequate standard coronal images, and hip morphology was classified according to the Graf classification system. Graf type I morphology was defined by an α angle of ≥60°. In the present cohort, the minimum measured α angle was 61°. Graf type Ia and Ib hips were not analyzed separately because beta-angle-based subclassification was not considered clinically relevant to the primary objective of the present study; therefore, both subtypes were categorized as Graf type I.

Both hips were evaluated independently. Dynamic ultrasonographic stability assessment with posterior stress or other provocative maneuvers was not performed; all measurements were obtained without the application of stress. Measurements were performed only on images fulfilling the standard anatomical and technical criteria of the Graf method.

Radiographic Examination

An AP pelvic radiograph was obtained with the infant in the supine position. Both lower extremities were positioned symmetrically with the hips in a neutral position and the patellae oriented anteriorly to minimize rotational error. Care was taken to ensure pelvic symmetry by aligning the iliac wings and obturator foramina. Radiographic technical adequacy was assessed before acetabular measurements were performed. Pelvic positioning was considered acceptable when the obturator foramina and iliac wings were approximately symmetric, the sacrum and coccyx were aligned with the pubic symphysis, and pelvic inclination permitted appropriate visualization of the acetabular landmarks. Radiographs demonstrating substantial pelvic rotation, pelvic obliquity, excessive lordosis, abnormal pelvic inclination, or other positioning errors that could interfere with reliable identification of the Hilgenreiner line, the acetabular roof, or the lateral acetabular margin were considered technically inadequate for quantitative assessment. No predefined numerical cutoff for the sacrococcygeal-pubic symphysis distance was used. No radiographs were excluded for inadequate positioning, nor did any examinations require repeat acquisition for technical inadequacy. The radiograph, which included the entire pelvis and proximal femora, was acquired using a standardized pediatric low-dose imaging protocol appropriate for infants. Pelvic radiographs were evaluated using the Hilgenreiner, Perkin, and Shenton reference lines. The acetabular angle was measured separately for the right and left hips. For patient-level statistical analysis, the higher of the two measurements was used to represent the individual patient. The acetabular angle was also measured to provide a quantitative assessment of acetabular development. Demographic characteristics, including age and sex, were recorded. In addition, the presence of established DDH-related risk factors other than family history was documented.

Radiographic Definition of Dysplasia

Radiographic assessment was based on the acetabular angle, the relationship of the femoral head to the Hilgenreiner and Perkin lines, and the continuity of the Shenton line. Because acetabular development is age dependent, acetabular angle measurements were interpreted according to published age-appropriate reference values rather than a single fixed threshold. Age-, sex-, and side-specific normative values reported for the pediatric population (CIs) were used as the reference for interpretation.[11]

For radiographic classification, isolated acetabular dysplasia was defined as an acetabular angle exceeding the age-appropriate reference range, with a concentrically positioned femoral head and a preserved Shenton line. Subluxation was defined as partial displacement of the femoral head from its expected relationship with the acetabulum, accompanied by abnormal femoral head position and/or disruption of the Shenton line without complete dislocation. Dislocation was defined as a complete loss of the normal femoral head-acetabular relationship, with displacement from the expected inferomedial quadrant, as defined by the Hilgenreiner and Perkin lines.

Femoral head position was assessed using the Hilgenreiner and Perkin reference lines and the Shenton line; a separate quantitative femoral head coverage measurement was not performed. Symmetry of the ossific nucleus was not used as a predefined quantitative diagnostic criterion.

Methods-Risk-Factor Classification

In addition to a positive family history, other documented DDH-related factors were recorded, including female sex, breech presentation, first-born status, multiple pregnancy, and associated musculoskeletal or anatomical abnormalities such as torticollis. Because positive family history was an inclusion criterion, all children in the study had this baseline risk factor. Patients with multiple additional documented DDH-related factors were evaluated separately as a higher-risk subgroup.

Primary Outcome

The primary outcome was the detection of any DDH-related abnormality on follow-up imaging during the available follow-up period. On follow-up ultrasonography, an abnormal finding was defined as a hip morphology other than Graf type I. On pelvic radiography, an abnormal finding was defined as one or more of the following: an acetabular angle exceeding the age-appropriate reference range, disruption of the Shenton line, or abnormal femoral head position relative to the Hilgenreiner and Perkin lines. Radiographic abnormalities were further categorized, when applicable, as isolated acetabular dysplasia, subluxation, or dislocation according to these predefined radiographic criteria. Physical examination findings were recorded as complementary clinical data but not included as a separate component of the primary imaging outcome.

Sample Size and Precision Analysis

Because the study was retrospective, no a priori sample size calculation was performed. All patients who met the predefined eligibility criteria during the study period and had available follow-up imaging were included. To quantify the precision of the zero-event outcome, an exact 95% binomial confidence interval was calculated for the observed event proportion.

Statistical Analysis

All study variables were initially recorded on standardized data collection forms and subsequently transferred to a Microsoft Excel database. Data entries were rechecked to minimize potential transcription errors. Statistical analyses were performed using IBM SPSS Statistics for Windows, version 20.0.

The distribution of continuous variables was assessed using the Kolmogorov-Smirnov test. Normally distributed numerical variables were presented as mean ± standard deviation, whereas non-normally distributed variables were summarized as median and interquartile range. Comparisons of continuous variables between groups were performed using the independent-samples Student's t test for normally distributed data and the Mann-Whitney U test for non-normally distributed variables.

Exact binomial 95% confidence intervals were calculated for the principal proportions reported in the study.

Results

The medical records and imaging data of 842 children who underwent ultrasonographic screening for DDH were retrospectively reviewed. After applying the predefined eligibility criteria, 243 children constituted the final study population (Figure 1).

The mean age of the study population was 10.3 months ±3.1 weeks. The cohort consisted of 172 girls (70.8%) and 71 boys (29.2%). The repeat-ultrasonography group included 60 girls (67.4%) and 29 boys (32.6%); the radiography group included 112 girls (72.7%) and 42 boys (27.3%). There was no significant difference in sex distribution between the two groups (p=0.380).

Initial ultrasonographic examinations were performed at a median age of 8.6 weeks (range, 6.5-12.4 weeks).

A total of 89 patients (36.6%) underwent repeat ultrasonography at a median age of 7.2 months (range, 6.2-12.4 months). None of these patients demonstrated abnormal findings on ultrasonography or physical examination during follow-up; all were considered normal (Figure 2).

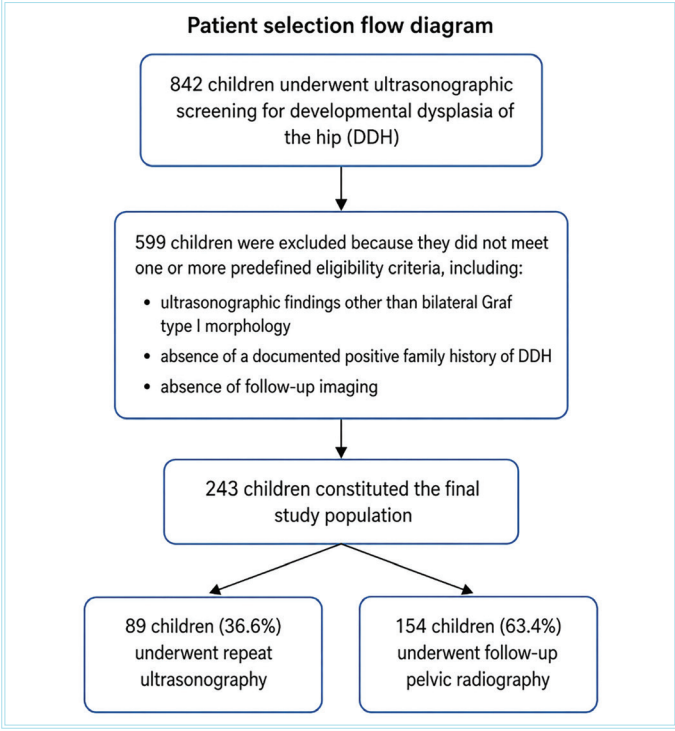

Figure 1. Patient-selection/STROBE flowchart

DDH: Developmental dysplasia of the hip

The remaining 154 patients (63.4%) underwent follow-up pelvic radiography at a median age of 8.5 months (range, 6.2-22.0 months). In all patients, the Shenton line was preserved, and the upper femoral epiphysis was located within the inferomedial quadrant defined by the Hilgenreiner and Perkin lines.

No cases meeting the predefined criteria for DDH were identified during the available follow-up period (0/243, 0%; 95% CI: 0%-1.51%).

The mean acetabular angle in the overall study population was 25.4±0.7°.

A representative AP pelvic radiograph demonstrating the radiographic landmarks and measurements used in the study, including the Hilgenreiner and Perkin lines, the preservation of the Shenton lines, the femoral head position within the inferomedial quadrants, and the bilateral acetabular angle measurements, is shown in Figure 3.

Seven patients (2.9%) underwent two follow-up radiographic examinations. Among these patients, five had multiple DDH-related risk factors. The acetabular angles measured on the first radiographs were relatively higher than those in the overall cohort but remained within the expected range for age. On subsequent examinations, all acetabular angles decreased, with final measurements below 21° (Table 1). None of the seven patients who underwent serial radiographic follow-up received an abduction brace or other orthopedic treatment; all were managed with observation.

Nine patients had multiple DDH-related risk factors (Table 2). Among these patients, five underwent more than one follow-up radiographic

Table 1. Patients who underwent two follow-up radiographic examinations

Patient no	1st acetabular angle (°)	2nd acetabular angle (°)
1	27.7	20.8
2	28.5	20.8
3	28.0	19.1
4	28.3	20.0
5	28.0	19.9
6	28.5	20.4
7	28.3	20.7

Table 2. Patients with multiple risk factors

Patient no	Risk factors	Acetabular angle (°)
1	BP, F	26.1
2	BP, F	24.8
3	BP, F, DB	28.5
4	F, BP	24.2
5	BP, F, DB	28.3
6	BP, F	26.2
7	F, BP, DB	24.9
8	BP, F	28.4
9	BP, F, DB	24.1

It referred to a complicated delivery requiring additional obstetric intervention, defined as a delivery in which mechanical or fetal factors, such as fetal macrosomia, cephalopelvic disproportion, or shoulder dystocia, necessitated additional obstetric intervention, including vacuum- or forceps-assisted delivery or cesarean delivery
BP: Breech presentation, F: Female sex, DB: Difficult birth

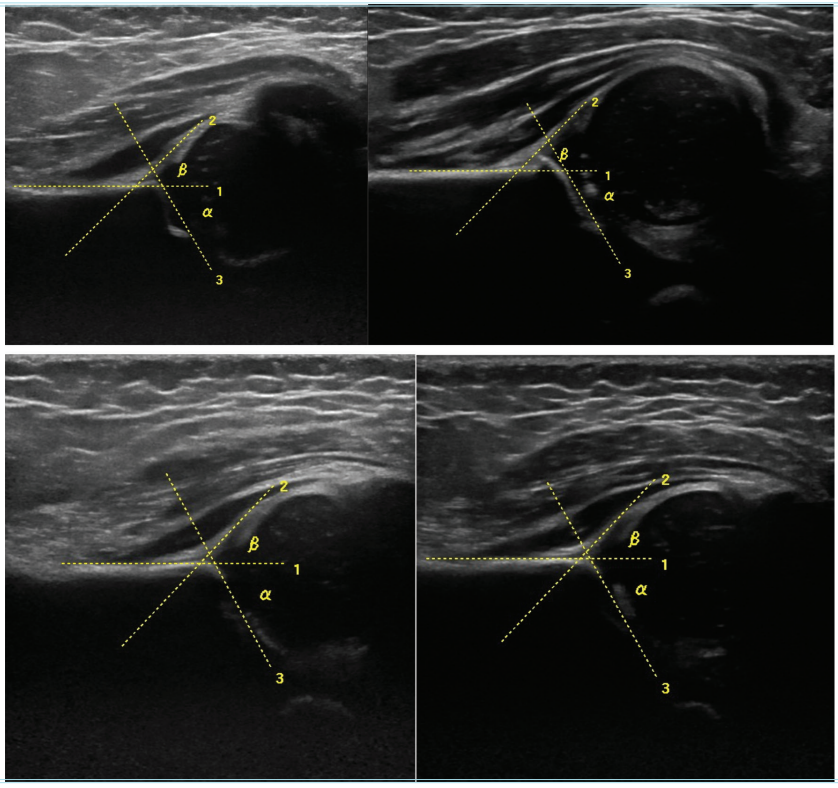

Figure 2. The alpha and beta angles were measured using the Graf method in the different patient groups presented above. The alpha angle values were greater than 60° in all groups

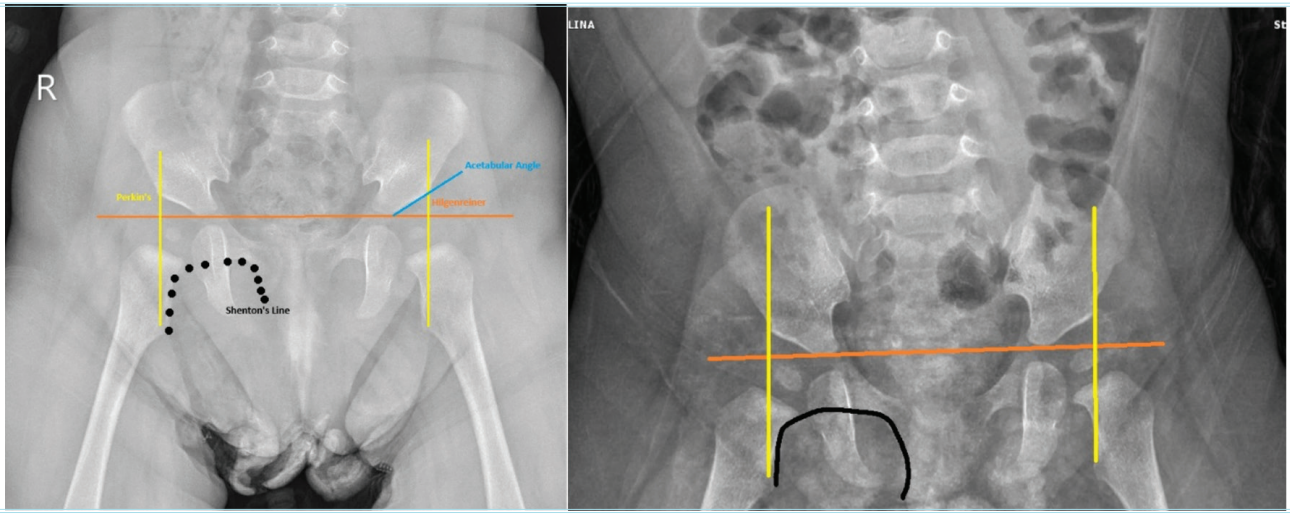

Figure 3. Representative anteroposterior pelvic radiograph demonstrating the radiographic assessment performed in the study. Anteroposterior pelvic radiograph of a a certain month-old child showing the Hilgenreiner lines, Perkin lines, and the inferomedial quadrants used to evaluate femoral head position. The Shenton lines are preserved bilaterally. The right and left acetabular angles are measured between the Hilgenreiner line and the acetabular roof line extending from the triradiate cartilage to the lateral acetabular margin. The anatomical landmarks and measurement lines used for calculation of the acetabular angles are indicated

examination. The mean acetabular angle in patients with multiple risk factors was slightly higher than that of the overall study population (26.2±1.8° vs. 25.4±0.7°); however, this difference was not statistically significant (p>0.05).

No cases meeting the predefined criteria for DDH were identified during the available follow-up period (0/243, 0%); the exact binomial 95% CI for the event rate was 0% to 1.51%.

Discussion

The principal finding of the present study was the absence of DDH-related abnormalities during the available follow-up period among children with a positive family history who had normal initial ultrasonographic findingsthat, among children with a positive family history and normal initial ultrasonographic findings, no DDH-related

abnormalities were detected during the available follow-up period. None of the patients who underwent repeat ultrasonography demonstrated abnormal imaging or physical examination findings, and no pathologic hip configuration was identified among those evaluated with follow-up pelvic radiography. In addition, the Shenton line was preserved, and the upper femoral epiphysis was located within the expected inferomedial quadrant in all radiographically assessed patients. These findings suggest that, although a positive family history is clinically relevant during initial risk stratification, its isolated presence may have limited value as an indication for routine repeated imaging after a technically adequate and normal early ultrasonographic examination.

Family history is a well-established risk factor for DDH and remains an important component of selective screening strategies.[1,5] Meta-analytic evidence has demonstrated a significant association between positive family history and DDH, while earlier ultrasonographic studies have also reported an increased frequency of abnormal neonatal hip findings among infants with recognized risk factors.[5,12] However, a distinction should be made between factors that increase the pretest probability of DDH at initial screening and those that independently predict late dysplasia after normal early imaging. The latter association appears considerably less certain. Arumilli et al.[6] found little support for routine secondary radiologic surveillance solely on the basis of family history after reassuring early assessment, and similar conclusions were reported by Osarumwense et al.[7] and Tafazal and Flowers.[8] Our findings are consistent with these studies and reinforce the concept that family history may be more informative in determining who should undergo initial imaging than in identifying who requires indefinite follow-up after a normal examination.

The present findings are also consistent with our previous study, in which no late DDH was detected among 205 children with a positive family history and normal initial ultrasonographic findings.[9] The current cohort, comprising a larger study population, provides further support for that observation and demonstrates a similarly low diagnostic yield of repeated imaging. This consistency is clinically relevant because the available literature remains heterogeneous regarding follow-up schedules, imaging modalities, and definitions of radiographic dysplasia. Price et al.,[10] in a large selective screening program, also reported a very low yield of abnormal radiographic findings following normal initial ultrasonography. Taken together, these findings argue against an automatic policy in which every infant with a family history undergoes repeated ultrasonography or pelvic radiography, irrespective of the quality and result of the initial examination. Nevertheless, this interpretation should not be extended indiscriminately to all high-risk infants, particularly because different risk factors may not carry equivalent prognostic implications.

The predominance of girls in our cohort is consistent with the recognized epidemiologic profile of DDH. Female sex has repeatedly been associated with an increased risk of abnormal hip development and is frequently included among the major variables used for selective screening.[5,12] In the present study, girls constituted 70.8% of the population. This distribution may reflect both the underlying biological association and referral patterns in clinical practice. However, the predominance of female patients did not translate into detectable late DDH after a normal initial ultrasonography. This observation further illustrates that the presence of an established epidemiologic risk factor does not necessarily indicate persistent structural abnormality when early imaging demonstrates normal hip morphology. Clinical and ultrasonographic assessments are complementary rather than interchangeable, and discrepancies between them have previously been documented in neonatal screening cohorts.[13] Therefore, the reassuring implications of a normal ultrasound depend on technically appropriate image acquisition and interpretation.

Another important finding was the radiographic behavior of the acetabular angle. The mean acetabular angle in the overall cohort was 25.4±0.7°, while patients with multiple risk factors demonstrated a slightly higher mean value of 26.2±1.8°. However, this difference was not statistically significant. Moreover, among patients who underwent more than one radiographic examination, the initially higher acetabular angles decreased on subsequent imaging, reaching final values below 21°. This pattern is compatible with progressive acetabular maturation rather than persistent dysplasia. Interpretation of such measurements requires caution because acetabular parameters change with age and can be influenced by pelvic positioning, rotation, landmark identification, and measurement technique.[14] Consequently, a relatively high acetabular angle on a single examination—particularly when other radiographic relationships remain normal—should not automatically be interpreted as evidence of progressive DDH.

The spontaneous decrease in acetabular angles observed on serial radiographs also raises an important issue regarding over-surveillance. Minor or borderline radiographic deviations may prompt repeated examinations even when the overall hip configuration is normal. In our cohort, seven children underwent two follow-up radiographic examinations; despite relatively higher initial values, subsequent measurements showed improvement rather than deterioration. Similar concerns have been raised in previous studies evaluating later radiography after normal ultrasonography.[8-10] Radiography remains valuable after progressive ossification and provides a robust assessment of osseous acetabular development, whereas ultrasonography offers direct evaluation of cartilaginous structures during early infancy.[3,15] These modalities should therefore be regarded as age-dependent and complementary tools, rather than tests that must routinely be performed sequentially on every at-risk infant. The low diagnostic yield observed in our cohort supports a more selective imaging strategy, particularly when early ultrasonography is normal and serial clinical examinations remain reassuring.

The subgroup with multiple risk factors deserves specific consideration. Nine patients in our cohort had more than one DDH-related risk factor, and their mean acetabular angle was numerically higher than that of the overall population, although the difference did not reach statistical significance. This finding may indicate either a true but small cumulative effect or simply random variation resulting from the limited size of this subgroup. Previous literature supports the importance of risk-based assessment but does not establish that all combinations of risk factors confer the same probability of persistent or late dysplasia.[5,12] Accordingly, our data do not justify routine prolonged surveillance for every child with multiple risk factors, but they also do not exclude the possibility that selected combinations—particularly those involving stronger mechanical risk factors—may warrant individualized follow-up. Larger cohorts with sufficient numbers in each risk-factor combination are required to determine whether cumulative risk models outperform single-factor approaches.

From a practical perspective, the present findings support a distinction between indications for initial screening and indications for post-screening surveillance. Family history is a reasonable indication

for careful clinical assessment and early ultrasonography,[1,5] but the persistence of this historical risk factor after a normal high-quality scan does not necessarily imply continued structural risk. Such a distinction could reduce unnecessary repeat appointments, radiographic exposure, healthcare utilization, and parental anxiety. This concept is also aligned with the broader movement toward selective ultrasound-first imaging pathways in which radiography is reserved for cases with persistent uncertainty or specific clinical indications, rather than being applied automatically to all screened infants. Recent technical research has explored selective escalation of imaging from ultrasonography to radiography as a radiation-sparing strategy, although such approaches still require clinical validation before routine implementation.

Study Limitations

The present study has several limitations. First, its retrospective design introduces the possibility of selection bias and limits control over imaging intervals and follow-up protocols. The study did not include a control group of children without a positive family history of DDH nor comparison groups of children with other isolated DDH-related risk factors. Therefore, the present findings cannot determine whether the observed follow-up outcomes differ from those of the general screened population or from those of children with alternative individual risk profiles. Second, follow-up was not uniform: some children underwent repeat ultrasonography, whereas others were assessed with pelvic radiography. Although this reflects real-world clinical practice, modality heterogeneity complicates direct comparison between follow-up pathways. Third, the subgroup with multiple risk factors was small, limiting statistical power to detect modest differences in acetabular angle. Fourth, interobserver and intraobserver agreements for ultrasonographic classification and radiographic measurements were not assessed. This is relevant because both Graf classification and acetabular measurements may be affected by image acquisition, landmark selection, and observer experience.[13,14,16] Fifth, the duration of follow-up may not be sufficient to exclude all forms of very late acetabular dysplasia. Therefore, the absence of detected late DDH should not be interpreted as proof of zero lifetime risk. Finally, the degree of familial relationship and the severity of DDH in affected relatives were not stratified; these variables may modify hereditary risk and should be addressed in future studies.

Despite these limitations, the study has clinically relevant implications. The relatively large cohort of children with a positive family history, the inclusion of both ultrasonographic and radiographic follow-up data, and the assessment of acetabular development provide a pragmatic evaluation of a common surveillance dilemma. Our findings indicate that routine, repeated imaging after a normal initial ultrasound has a very low diagnostic yield in children whose principal risk factor is a family history. Accordingly, follow-up decisions should be individualized and incorporate the quality of the initial examination, serial physical findings, the presence and combination of additional risk factors, and any emerging clinical concern, rather than family history alone.

Conclusions

The findings of the present study suggest that a positive family history is an important criterion for initial DDH risk assessment but may not, in isolation, justify routine, repeated ultrasonography or pelvic radiography after a normal early ultrasonographic examination. The absence of detected DDH-related abnormalities during the available follow-up period, together with the progressive normalization of relatively high acetabular angles on serial imaging, supports a more selective follow-up strategy. Prospective studies with standardized imaging intervals, predefined radiographic thresholds, longer follow-up periods, and adequately powered subgroups defined by combined risk factors are needed to identify the small subset of children who may genuinely benefit from continued surveillance.

Ethics

Ethics Committee Approval: Ethical approval for this study was obtained from the Erzincan Binali Yıldırım University Clinical Research Ethics Committee (approval no: EBYU-KAEK-2025-21/16, date: 27.11.2025).

Informed Consent: Since the study was a retrospective study, informed consent was not required by the ethics committee.

Footnotes

Authorship Contributions

Concept: O.A., Design: E.A., B.A.E., Data Collection or Processing: O.A., Analysis or Interpretation: E.A., Literature Search: E.A., Writing: E.A.

Conflict of Interest: No conflict of interest was declared by the authors.

Financial Disclosure: The authors declared that this study received no financial support.

References

1. Shaw BA, Segal LS; SECTION ON ORTHOPAEDICS. Evaluation and referral for developmental dysplasia of the hip in infants. Pediatrics. 2016;138:e20163107.
2. Shipman SA, Helfand M, Moyer VA, Yawn BP. Screening for developmental dysplasia of the hip: a systematic literature review for the US preventive services task force. Pediatrics. 2006;117:e557-76.
3. Expert Panel on Pediatric Imaging; Nguyen JC, Dorfman SR, Rigsby CK, et al. ACR appropriateness criteria® developmental dysplasia of the hip-child. J Am Coll Radiol. 2019;16:S94-103.
4. Holen KJ, Tegnander A, Bredland T, et al. Universal or selective screening of the neonatal hip using ultrasound? A prospective, randomised trial of 15,529 newborn infants. J Bone Joint Surg Br. 2002;84:886-90.
5. Ortiz-Neira CL, Paolucci EO, Donnon T. A meta-analysis of common risk factors associated with the diagnosis of developmental dysplasia of the hip in newborns. Eur J Radiol. 2012;81:e344-51.
6. Arumilli BR, Koneru P, Garg NK, et al. Is secondary radiological follow-up of infants with a family history of developmental dysplasia of the hip necessary? J Bone Joint Surg Br. 2006;88:1224-7.
7. Osarumwense D, Popple D, Kershaw IF, Kershaw CJ, Furlong AJ. What follow-up is required for children with a family history of developmental dysplasia of the hip? J Pediatr Orthop B. 2007;16:399-402.
8. Tafazal S, Flowers MJ. Do we need to follow up an early normal ultrasound with a later plain radiograph in children with a family history of developmental dysplasia of the hip? Eur J Orthop Surg Traumatol. 2015;25:1171-5.
9. Aydin S, Fatihoglu E. Family history in developmental dysplasia of the hip: should we follow-up? Eur Res J. 2019;5:957-61.
10. Price KR, Dove R, Hunter JB. The use of X-ray at 5 months in a selective screening programme for developmental dysplasia of the hip. J Child Orthop. 2011;5:195-200.

11. Akel I, Songur M, Karahan S, Yilmaz G, Demirkiran HG, Tumer Y. Acetabular index values in healthy Turkish children between 6 months and 8 years of age: a cross-sectional radiological study. Acta Orthop Traumatol Turc. 2013;47:38-42.
12. Bache CE, Clegg J, Herron M. Risk factors for developmental dysplasia of the hip: ultrasonographic findings in the neonatal period. J Pediatr Orthop B. 2002;11:212-8.
13. Kyung BS, Lee SH, Jeong WK, Park SY. Disparity between clinical and ultrasound examinations in neonatal hip screening. Clin Orthop Surg. 2016;8:203-9.
14. Lee YK, Chung CY, Koo KH, Lee KM, Kwon DG, Park MS. Measuring acetabular dysplasia in plain radiographs. Arch Orthop Trauma Surg. 2011;131:1219-26.
15. Keller MS, Nijs EL. The role of radiographs and US in developmental dysplasia of the hip: how good are they? Pediatr Radiol. 2009;39(Suppl 2):S211-5.
16. Thallinger C, Pospischill R, Ganger R, Radler C, Krall C, Grill F. Long-term results of a nationwide general ultrasound screening system for developmental disorders of the hip: the Austrian hip screening program. J Child Orthop. 2014;8:3-10.